Theor Appl Genet (2017) 130:819–839
DOI 10.1007/s00122-017-2854-z

ORIGINAL ARTICLE

SSR-enriched genetic linkage maps of bermudagrass (*Cynodon dactylon* × *transvaalensis*), and their comparison with allied plant genomes

Sameer Khanal[1] · Changsoo Kim[1,2] · Susan A. Auckland[1] · Lisa K. Rainville[1] · Jeevan Adhikari[1] · Brian M. Schwartz[3] · Andrew H. Paterson[1]

Received: 16 September 2016 / Accepted: 4 January 2017 / Published online: 6 February 2017

Abstract

Key message **We report SSR-enriched genetic maps of bermudagrass that: (1) reveal partial residual polysomic inheritance in the tetraploid species, and (2) provide insights into the evolution of chloridoid genomes.**

Abstract This study describes genetic linkage maps of two bermudagrass species, *Cynodon dactylon* (T89) and *Cynodon transvaalensis* (T574), that integrate heterologous microsatellite markers from sugarcane into frameworks built with single-dose restriction fragments (SDRFs). A maximum likelihood approach was used to construct two separate parental maps from a population of 110 F_1 progeny of a cross between the two parents. The T89 map is based on 291 loci on 34 cosegregating groups (CGs), with an average marker spacing of 12.5 cM. The T574 map is based on 125 loci on 14 CGs, with an average marker spacing of 10.7 cM. Six T89 and one T574 CG(s) deviated from disomic inheritance. Furthermore, marker segregation data and linkage phase analysis revealed partial residual polysomic inheritance in T89, suggesting that common bermudagrass is undergoing diploidization following whole genome duplication (WGD). Twenty-six T89 CGs were coalesced into 9 homo(eo)logous linkage groups (LGs), while 12 T574 CGs were assembled into 9 LGs, both putatively representing the basic chromosome complement ($x=9$) of the species. Eight T89 and two T574 CGs remain unassigned. The marker composition of bermudagrass ancestral chromosomes was inferred by aligning T89 and T574 homologs, and used in comparisons to sorghum and rice genome sequences based on 108 and 91 significant blast hits, respectively. Two nested chromosome fusions (NCFs) shared by two other chloridoids (i.e., zoysiagrass and finger millet) and at least three independent translocation events were evident during chromosome number reduction from 14 in the polyploid common ancestor of Poaceae to 9 in *Cynodon*.

Communicated by Thomas Lubberstedt.

Electronic supplementary material The online version of this article (doi:10.1007/s00122-017-2854-z) contains supplementary material, which is available to authorized users.

✉ Andrew H. Paterson
paterson@uga.edu

[1] Plant Genome Mapping Laboratory, University of Georgia, Athens, GA 30602, USA

[2] Department of Crop Science, Chungnam National University, 99 Daehak-ro, Yuseong-gu, Daejeon 34134, South Korea

[3] Department of Crop and Soil Sciences, University of Georgia, Tifton, GA 31793, USA

Introduction

The genus *Cynodon* represents several perennial grasses that are widespread in tropical and subtropical landscapes, and commonly referred to as bermudagrass. Common bermudagrass [*Cynodon dactylon* (L.) Pers.] was introduced into the United States in the mid-1700's and within decades, it naturalized in the warm regions of the country, becoming the most prominent pasture grass of the Southern states (Harlan 1970; Wu 2011). The *Cynodon* genus carries a suite of important characteristics that make it suitable for multifaceted end-uses with huge economic and ecological significance. Its resilience and fast recuperative potential, perenniality and aggressive sod-forming growth habit, and high resource use efficiency makes it an excellent multipurpose species that is widely used as a lawn and sports turf (e.g., on football fields and golf courses), livestock

feed (i.e., for hay, forage, and pasture), and ground cover (i.e., to stabilize ditchbanks, roads, levees, and marginal lands). Ironically, these same characteristics render it invasive, highly competitive, and an expensive weed to manage. Recently, bermudagrass has attracted research interest as a biomass feedstock for biofuel production (Xu et al. 2011), as a phytoremediation agent for soil reclamation from heavy metals (Elekes et al. 2010), petroleum (Razmjoo and Adavi 2012) and salinity (Cerda et al. 2007); and as a medicinal plant for its pharmacognostic properties (Rai et al. 2010).

Bermudagrass is a highly heterozygous and largely self-incompatible outcrossing plant (Burton and Hart 1967; Tan et al. 2014) with C4 photosynthesis and an estimated average 1X genome size of ~540 Mbp (Bethel et al. 2006; Taliaferro et al. 1997). *Cynodon* spp., including common bermudagrass, exhibit a series of ploidy levels (de Wet and Harlan 1970; Gulsen et al. 2009; Kang et al. 2008; Wu et al. 2006) with a basal chromosome number of 9 (Forbes and Burton 1963; Harlan et al. 1970). A number of leading turf varieties are sterile triploid hybrids from crosses between tetraploid common bermudagrass (*C. dactylon* L. Pers. var. *dactylon*) and a diploid African bermudagrass (*C. transvaalensis* Burtt Davy). Current varietal development is largely focused on tetraploid cytotypes ($2n=4x=36$) for forage and pasture, while both tetraploid and triploid cytotypes ($2n=3x=27$) are used in turf breeding (Wu 2011).

The genus *Cynodon* belongs to family *Poaceae* (*Gramineae*) and subfamily *Chloridoideae*, in the "PACC" clade that also contains subfamilies *Panicoideae, Arundinoideae*, and *Centothecoideae* (Kim et al. 2009). *Panicoideae* including maize, sorghum, sugarcane, and foxtail millet have been extensively studied, but other *Poaceae* subfamilies lag in scientific exploration. In particular, only a handful of the more than 1,300 chloridoids have attracted genome-wide exploration, which significantly limits our understanding of their evolutionary history and our ability to exploit molecular breeding tools for their improvement. Among the four most important genera within *Chloridoideae, Cynodon* (including bermudagrass) and *Eleusine* (finger millet) are in the same clade (i.e., subtribe Eleusininae), *Zoysia* (zoysiagrass) is in a sister clade, and *Eragrostris* (tef) is sister to both (Peterson et al. 2010a; Soreng et al. 2015). Currently, *Cynodon* lags behind these three other chloridoid genera in genomics and molecular breeding applications.

While bermudagrass molecular marker research has shed some light on genetic diversity (Harris-Shultz et al. 2011; Kamps et al. 2011; Kang et al. 2008; Ling et al. 2012; Wu 2011; Wu et al. 2004, 2006; Zhiyong et al. 2013), information on structural genomics is critically low. Little is known about bermudagrass genome constitution and evolution (i.e., origin, nature of polyploidy, duplication and divergence), and chromosome behavior during meiosis (i.e., inheritance), each of which are important for evolutionary studies, genetic linkage analysis, quantitative trait loci (QTL) detection, and crop improvement. To date only three papers have reported the construction of genetic linkage maps in bermudagrass, two of which report addition of small numbers of EST-derived markers to the only available framework. The first genetic linkage framework of bermudagrass (*C. dactylon* × *transvaalensis*) (Bethel et al. 2006) was based on single-dose restriction fragments (SDRFs) (Wu et al. 1992) generated from probes based on bermudagrass genomic clones and heterologous cDNAs from *Pennisetum* and rice. Triploid ($2n=3x=27$) F_1 progeny were used for mapping, based on heterozygosity within each parent, following a pseudo-testcross mapping strategy (Grattapaglia and Sederoff 1994). The T89 map was based on 155 SDRFs and 17 double-dose restriction fragments (DDRFs), while that of T574 was based on 77 SDRFs. Harris et al. (2010b) added twenty-one bermudagrass-resistance gene analogs (BRGA) and EST-SSRs to the published (Bethel et al. 2006) SDRF framework. The group further updated the map with an addition of 28 EST-SSRs mined from cDNA pseudo-molecules developed at Plant Genome Mapping Laboratory (Kim et al. 2008). Further, based on disomic segregation of fourteen EST-SSRs and almost disomic profile at yet another marker locus (single inconsistent progeny), Harris-Shultz et al. (2010a) suggested that basic chromosomes pair preferentially during meiosis and that tetraploid bermudagrass (i.e., T89) could be a segmental polyploid. Recently, Guo et al. (2015) proposed allopolyploidy of common bermudagrass based on marker segregation analysis and Gong et al. (2013) made the same proposal based on fluorescence in situ hybridization (FISH) and meiotic chromosome configurations.

The genome of another chloridoid, tef [*Eragrostis tef* (Zucc.) Trotter], has been sequenced (Cannarozzi et al. 2014), but due to lack of a complete and saturated linkage map, comparative genomic assessment was inadequate to delineate chromosomal rearrangements during its evolution. However, high-density sequence-tagged genetic maps of zoysiagrass (Huang et al. 2016; Wang et al. 2015a) and finger millet (Srinivasachari et al. 2007) have yielded novel insights into chloridoid genome evolution. Densely populated sequence-tagged saturated linkage maps are needed to improve knowledge of genome structural diversity in *Poaceae* that lack genome sequences. Accordingly, a genetic linkage map in prairie cordgrass (*Spartina pectinate* Link), another chloridoid with bioenergy potential, was constructed and compared with sorghum based on homologous tef genome scaffolds (Crawford et al. 2016). Furthermore, high-resolution genetic maps can improve genome assembly by anchoring de novo sequences and providing a framework to orient and order smaller scaffolds

into chromosome-scale pseudomolecules (Bartholomé et al. 2015b; Fierst 2015). For example, the validity of second chloridoid genome to be sequenced and assembled (i.e., *Zoysia japonica* accession 'Nagirizaki') was authenticated and pseudo-chromosomes of the species were constructed (Tanaka et al. 2016) based on genetic linkage map from Wang et al. (2015a). However, no finished chloridoid genomes are reported; nevertheless, draft genomes are publicly available.

The development of linkage maps for many outcrossing species, including the framework linkage map of bermudagrass, relied on the "pseudo-testcross" strategy (Grattapaglia and Sederoff 1994) that involves separate estimation of parental linkage phases and recombination fractions, often using MapMaker/Exp (Lander et al. 1987). Wu et al. (2002) developed maximum-likelihood methods for simultaneous estimation of linkage and linkage phases, which have been successfully applied to several outcrossing species including sugarcane (Garcia et al. 2006; Oliveira et al. 2007; Palhares et al. 2012), passion fruit (Oliveira et al. 2008; Pereira et al. 2013), rubber tree (Souza et al. 2011), eucalyptus (Bartholomé et al. 2015a), and switchgrass (Lowry et al. 2015).

In the current study, application of a maximum-likelihood approach was extended to bermudagrass using functions implemented in the R software package OneMap (Margarido et al. 2007). We report the construction of complete SSR-enriched linkage maps of two bermudagrass species, *C. dactylon* × *C. transvaalensis* using the same full-sib progeny used to construct the RFLP-based framework (Bethel et al. 2006) and present an inferred ancestral chromosome complement based on alignment of the parental maps. Further, we leverage molecular approaches to assess the nature of ploidy in the tetraploid parent (i.e., T89). Additionally, we report comparative analysis with grass genome models (i.e, sorghum and rice) and four chloridoid species [i.e., tef (Cannarozzi et al. 2014), prairie cordgrass (Crawford et al. 2016), finger millet (Srinivasachari et al. 2007), and zoysiagrass (Wang et al. 2015a)] and deduce rearrangements that differentiate the modern *Cynodon* chromosomes from those of the polyploid common ancestor of Poaceae.

Materials and methods

Mapping population

A population of 113 F_1 hybrids from a cross between *C. dactylon* (T589; 4×) and *C. transvaalensis* (T574; 2×) developed by W. Hanna (University of Georgia, Tifton, GA) formed the basis of the framework linkage map (Bethel et al. 2006). Harris-Shultz et al. (2010a) verified diploid, triploid, and tetraploid ploidy levels of T574, the F_1s, and T89 genotypes, respectively. The two parents represent the two species crossed to produce several leading bermudagrass cultivars, including Tifgreen (Hein 1961; Robinson and Latham 1956) and Tifway (Burton 1960).

Genomic DNA and molecular marker resources

Extraction of genomic DNA followed Chittenden et al. (1994) as reported by Bethel et al. (2006). In a prior study, about 2500 simple sequence repeat (SSR) PCR primers from sugarcane expressed sequence tags (ESTs) were assayed for transferability and reproducibility in bermudagrass (our unpublished data). For a subset of about 300 markers, informative segregation and parental sources of each polymorphic band were ascertained in ten pseudo-testcross progenies. Thereafter, the presence and absence of each polymorphic band was visually determined and recorded for 95 additional F_1 individuals in the mapping population. All polymerase chain reactions (PCRs) were performed in 96-well plates, using 1 µL each of $MgCl_2$ (3 mM), dNTPs (2 mM), and 10× PCR buffer (100 mM Tris–HCL at pH 9, 500 mM KCL, and 15 mM $MgCl_2$), 0.2 µL of Taq DNA polymerase (1 U), 3.8 µL of ddH_2O, and 2 µL of template DNA (15 ng/µL) for a total volume of 10µL. The typical cycling conditions for PCR were 95 °C for 4 min in the first step, followed by 6 cycles of 94 °C for 40 s, a gradient reaction from 58 to 52 °C each for 1 min, and 72 °C for 1 min. The third step was set for 35 cycles of 94 °C for 40 s, 55 °C for 1 min, and 72 °C for 1 min. After the last cycle, reactions were incubated at 72 °C for final extension period of 10 min before cooling to 4 °C. PCR amplicons were resolved by 10% nondenaturing polyacrylamide gel electrophoresis, and visualized by staining with silver nitrate (Bassam et al. 1991).

Segregation analysis

Since different genotypic configurations are possible in segregating populations of a polyploid species, phenotype of a DNA marker is not adequate to define genotype at the underlying locus; rather, its segregation ratio across the progenies provides that information (Sorrells 1992; Wu et al. 1992). Following Wu et al. (1992), single-dose and biparental markers were tested by Chi-squared analysis for goodness of fit ($P = 0.01$) with 1:1 and 3:1 ratios expected for simplex (single copy) by nulliplex (no copy) and simplex by simplex markers, respectively. Next, parent specific double-dose (two copies) amplicons from the subgenomes, or paralogous copies of segmental duplications segregating in a 3:1 ratio were identified. Further, tetrasomic segregation ratios for duplex (two copies) by nulliplex (5:1) and duplex by simplex (11:1) markers were also tested,

following Ripol et al. (1999). Restriction fragment length polymorphism (RFLP) data for a total of 113 F_1 individuals were obtained from Bethel et al. (2006) and were pooled with SSR data for linkage analysis. Allelic SSRs and RFLPs showing disomic segregation were scored and analyzed as codominant markers. TetraploidMap (Hackett et al. 2007) was used to verify marker dosage classification and to examine significant simplex-duplex linkages.

Linkage analysis

The analyses were carried out following procedures proposed by Wu et al. (2002b) and implemented in OneMap software (Margarido et al. 2007). First, EM algorithm-based two-point pair-wise analysis was carried out between all pairs of markers (Dempster et al. 1977), which simultaneously estimated recombination fractions and linkage phases between marker-pairs based on posterior probabilities of Bayes' theorem ('rf.2pts' command). CGs were established with a minimum LOD (logarithm of odds ratio) threshold of 4.8 and a maximum recombination fraction $\theta = 0.4$ [the maximum detectable recombination fraction under autopolyploidy in a population of 113 individuals, following Wu et al. (1992)]. Map units (cM) were calculated by the method of Kosambi (1944). Clusters of linked markers or CGs were then ordered using a step-wise approach outlined in the OneMap tutorial. In short, for CGs constituting up to 7 markers, all possible marker orders were evaluated ('compare' command) while for the groups with more than 7 markers, a subset of six to seven informative markers were ordered to build frameworks to which other markers were individually tested ('try.seq' command). Once the CGs were built, unlinked markers were tried at LODs as low as 2 ('try.seq' command). Spurious associations were detected using recombination fraction vs. LOD heatmap plots for individual CGs. The final positions of the markers were refined using ripple search (Lander et al. 1987). Instead of integrating markers that fit arbitrary orders (using 'force' command), but are significantly linked with two or more safely ordered markers within the CGs, such markers were identified as accessory markers to their closest linkages. Fragmented LGs were identified based on weak linkages between one or more markers mapped to two or more CGs but which could not be unambiguously merged together, further supported by homology with rice and sorghum genomes. Comparative map length analyses were adjusted for the markers that were in the framework, but could not be mapped in the current study. Accordingly, two separate genetic linkage maps were built, one of each parental species.

TetraploidMap software was used to detect and verify simplex–duplex linkages in both coupling and repulsion phases and employed default Chi-squared tests with $P = 0.001$ (Hackett et al. 2007). In principle, a double dose marker (DDM) should be linked in coupling with two different CGs; ideally, these two CGs would comprise two homologous chromosomes in an autopolyploid (segregating in 5:1 ratio) or homoeologous chromosomes in an allopolyploid (segregating in 3:1 ratio). Nevertheless, a DDM could also represent a segmental duplication at non-homo(eo)logous regions (segregating in 3:1 ratio). In such cases, consistencies of identified chromosomal bridges were reconfirmed with shared multilocus probes, repulsion phase linkages, and homology with rice and sorghum genomes. Similarly, parental maps were aligned to infer ancestral chromosomes based on shared multilocus markers and biparental bridges, further supported by inferred homology with the allied plant genomes. All map charts were drawn using MapChart v2.1 (Voorrips 2002).

Marker distribution, estimated recombination length, and genome coverage

To examine marker distribution over the entire map, relationships between lengths (cM) of CG and numbers of markers in each CG were tested with Pearson correlation coefficients. For the estimation of genome length, two different approaches were implemented. First, the average marker spacing/interval (s) was calculated by dividing the total map length by the number of intervals (number of markers minus number of CGs). Then, the estimated genome length ($Ge1$) was determined by adding 2 s to the length of each CG (Fishman et al. 2001). Second, using Method 4 of Chakravarti et al. (1991), the expected genome size ($Ge2$) was estimated as the sum of the length of each CG multiplied by $(m+1)/(m-1)$, in which m is the number of markers on each CG. The total map length (G_0) was the sum of the length of each CG. To infer monoploid estimates (monoploid defined here as a map with LGs consistent with the basal chromosome number), both methods were adjusted to account for fragmented LGs. CGs not assigned to homologous groups (HGs) were also excluded from genome size and coverage estimates for putative monoploid maps. Coverage of the *Cynodon* genome by the linkage map was estimated by the ratio G_0/Ge, where Ge represents the average of the estimated genome lengths from the two approaches, respectively. Genome coverage was also calculated by:

$$c = 1 - e^{-2dn/G},$$

where c is the proportion of the genome within d cM of a marker, G is the estimated genome length, and n is the number of markers in the map (Lange 1982).

Mode of inheritance

A number of empirical approaches exist to suggest the type of inheritance (disomic/polysomic) in a polyploid species. Classical cytogenetic evidence involves meiotic chromosome pairing behavior (e.g., bivalent vs. multivalent chromosomal association) during meiosis to infer mode of inheritance (Müntzing 1936). Cytological evidence in *Cynodon* was reviewed. Furthermore, strictly disomic segregation of codominant markers suggests preferential pairing in a segmental or a complete allopolyploid (Guo et al. 2015). Marker segregation data was scanned for codominant segregants. Third, the ratio of simplex to multiplex markers may indicate allopolyploid (0.75:0.25) or autopolyploid (0.83:0.17) genome constitution (Silva et al. 1993). Chi-squared values were estimated to test the goodness of fit to different genome constitution ratios based on observed single-dose vs. multiple dose marker frequencies. Fourth, recombination fractions and linkage phases between all marker-pairs ('rf.2pts' command) were analyzed to estimate the ratio of markers in repulsion vs. coupling phase, a measure that indicates disomic, polysomic, or intermediate modes of inheritance (Sorrells 1992; Wu et al. 1992). Within established CGs, linkage estimates were accepted at LOD thresholds as low as 2. Deviations from 1:1 ratio (i.e., equal frequency as expected in a disomic inheritance) of repulsion vs. coupling, were tested using Chi-squared assays for individual CGs, as well as at genome-wise levels (Wu et al. 1992). Statistically significant deviations suggested random chromosome pairing while non-significant deviations suggested chromosome pairing to be preferential. Fifth, linkage between putative homo(eo)logous groups would indicate either complete (autopolyploidy) or partial (segmental polyploidy) random chromosome pairing during meiosis, which could result from different levels of preferential pairing. Two-point linkage data for all marker-pairs was scanned for coupling or repulsion linkages between markers mapped to homo(eo)logous groups. Between putative homo(eo)logous groups, linkage estimates were accepted at LOD thresholds as low as 2 and $\theta = 0.4$.

Comparative mapping

The sequences of mapped RFLP probes and ESTs corresponding to EST-SSRs were BLASTed against pseudomolecules of rice (*Oryza sativa* v 7.0) (Kawahara et al. 2013) and sorghum (*Sorghum bicolor* v2.1) (Paterson et al. 2009) using the Phytozome BLAST tool (http://phytozome.jgi.doe.gov) at a significance threshold $\leq 1 \times 10^{-10}$. The output was manually parsed to identify the most significant hits and their chromosomal locations. An ancestral chromosome consensus of bermudagrass homologs was built using MergedMap (Wu et al. 2011). Colinearity was inferred by comparing the chromosomal locations of the best rice and sorghum hits to the orders of the corresponding markers on the inferred *Cynodon* ancestral chromosomes. BLASTn (Altschul et al. 1997) implemented in Zoysia Genome Database (zoysia.kazusa.or.jp) was used to identify significant sequence homologies (at $\leq 1 \times 10^{-10}$) between bermudagrass markers and *Zoysia japonica* Nagirizaki pseudomolecules (Tanaka et al. 2016). For a comprehensive comparative assessment, studies pertinent to karyotype evolution in four chloridoid species [tef (Cannarozzi et al. 2014), prairie cordgrass (Crawford et al. 2016), finger millet (Srinivasachari et al. 2007), and zoysiagrass (Huang et al. 2016; Tanaka et al. 2016; Wang et al. 2015a)] were also compared with the current study. Chromosome nomenclature followed genus and species initials followed by established chromosome number [i.e., *Sorghum bicolor* Sb 1 to Sb 10; *Oryza sativa* Os 1 to Os 12; *Zoysia japonica* Zj 1 to Zj 20; *Zoysia mantrella Zm* 1 to *Zm* 20).

Results

Segregation analysis

A total of 116 SSR primer pairs from sugarcane ESTs amplified 240 segregating bands in bermudagrass parental samples and 105 F_1 progenies, of which 138 (57.5%) were T89-specific, 81 (33.7%) were T574-specific, and 21 (8.7%) were shared. Observed segregation ratios were calculated for a pooled dataset of 668 markers (240 SSRs and 428 RFLPs), which included a total of 21 biparental markers and 440 and 207 uniparental markers from T89 and T574, respectively. The classification of SSR and RFLP markers based on their segregation ratios is summarized in Table 1. In the tetraploid parent T89, 82.5% of undistorted markers were single dose and 17.5% were higher dose ($P = 0.01$). Interestingly, 11% of markers also satisfied double-dose ratios in the diploid parent T574 (see "Discussion"). Segregation distortion accounted for 12.1 and 9.3% of uniparental markers in T574 and T89, respectively. Three genotypes, namely B17-38, B17-39, and B17-107 showed erratic genotype patterns (for example, missing uniformly monomorphic bands, or absence of bands at codominant marker loci showing disomic segregation) for a number of markers. Since the biological basis of such occurrences were not clear (perhaps meiotic abnormalities), the three genotypes were removed from further analyses. Forty-five allelic pairs (27 T89 and 18 T574-specific) showed disomic segregation in the combined RFLP and SSR dataset, which included 14 SSR and 31 RFLP marker-pairs.

Table 1 Classification of marker inheritance in bermudagrass based on Chi-squared assays ($P=0.01$), following Wu et al. (1992)

Marker/classification	*C. transvaalensis* (T574)	*C. dactylon* (T89)	Bi-parental	Total
SSRs				
Single dose (1:1)	60	118		178
Biparental (3:1)			13	13
Double dose (3:1) or (5:1)		6		6
Double dose (8:1) or (11:1)			4	4
Segregation distorted	21	14	4	39
RFLPs[a]				
Single dose (1:1)	102	211		313
Double dose (3:1) or (5:1)	20	64		84
Segregation distorted	4	27		31
Total	207	440	21	668

[a]RFLPs were developed and used by Bethel et al. (2006)

Map construction

C. transvaalensis (2n – 2x – 18) T574 map

The T574 map was constructed based on 171 markers including 70 SSRs (50 dominant, 6 codominant, 12 biparental, and two codominant biparental) and 101 RFLPs (89 dominant and 12 codominant). A total of 125 loci were mapped with 52 SSRs (39 dominant, 6 codominant, 5 biparental, and 2 codominant biparental markers) and 73 RFLPs (61 dominant and 12 codominant) (Fig. 1). Of a total of 46 unlinked markers, 50% deviated from the expected segregation ratios ($P=0.05$). Based on two-point recombination fraction estimates, six unlinked markers were significantly linked (LOD $\geq$4.8, $\theta=0.4$) with six different CGs, but they could not be unambiguously integrated into the respected CGs and were, therefore, identified as accessory markers (not shown). Three originally mapped markers were excluded from the updated map as they could not be mapped at the minimum threshold set for linkage analysis.

The integrated RFLP-SSR map is composed of 14 CGs covering a total of 1,188.4 cM, with 125 loci separated by an average of 10.7 cM (Table 2). On average, CGs are defined by about 9 markers and covers 84.9 cM. In comparison, the framework linkage map covered a total of 973 cM with 77 markers separated by an average of 16.5 cM and each CG was defined by about 4 markers covering about 54 cM.

Six CGs were inferred to represent fragments of three larger LGs based on weak linkages between them. T574 7a-2/b-I and T574 5a/b are two fragments of the same LG based on 4 coupling and 4 repulsion linkages supported by an average LOD of 2.42. Similarly, two novel LGs T574 11* and T574 12* with 2 and 5 markers are associated with LGs T574 9 and T574 3a/b with average linkage support of 3.69 and 5.25, respectively. As such, the final linkage map consists of 11 LGs with 2 to 18 markers each. Nine LGs with a minimum of 9 markers represented the basic chromosome complement of bermudagrass—two CGs with 2 markers each could not be associated with the major LGs (Supplemental Table 1).

C. dactylon (2n – 4x – 36) T89 map

The T89 map was constructed based on 349 markers including 139 SSRs (114 dominant, 8 codominant, 13 biparental, and 4 codominant biparental) and 210 RFLPs (191 dominant and 19 codominant). A total of 291 loci were mapped with 113 SSRs (that includes 93 dominant, 7 codominant, 9 biparental, and 4 codominant biparental) and 178 RFLPs (160 dominant and 18 codominant) (Fig. 1). Of a total of 58 unlinked markers, 20 showed distorted segregation ratios and/or have more than 50% missing data. Eight originally mapped markers were excluded from the updated map since they either were not mapped at the minimum threshold set for linkage analysis or were misclassified as a single dose marker (i.e., RZ557c was a DDM). Comparative map length analyses were adjusted for the missing markers. About 50% of unlinked markers were identified as accessory markers based on significant two-point recombination fractions with the linked ones (not shown).

The integrated RFLP-SSR map of T89 is composed of 34 CGs covering a total of 3248.7 cM, with 291 marker loci separated by an average of 12.5 cM (Table 2). On average, CGs are defined by about 8.6 markers and cover ~96 cM. In comparison, the framework linkage map covered a total of 1837.3 cM, with 144 markers (136 dominant, 12 codominant) separated by an average distance of 15.3 cM and each CG was defined by about four markers and covered an average of 52.5 cM.

Based on weak linkages between the CGs, twenty-six CGs were inferred to represent 18 LGs representing 9 complete homo(eo)logous pairs—five CGs with 2 and three CGs with 3 markers could not be associated with the major LGs (Supplemental Table 1).

In partial summary, a total of 149 (129 dominant, 7 codominant, 9 biparental, and 4 codominant biparental) and 58 new loci (48 dominant and 10 codominant) were added to the framework linkage maps of T89 and T574, which increased Bethel et al. (2006) framework map lengths by 22% and 77%, respectively. Four and eight novel CGs, with 12 and 24 markers, together with 7 and 17 independent end-extension events (i.e., markers mapped to the

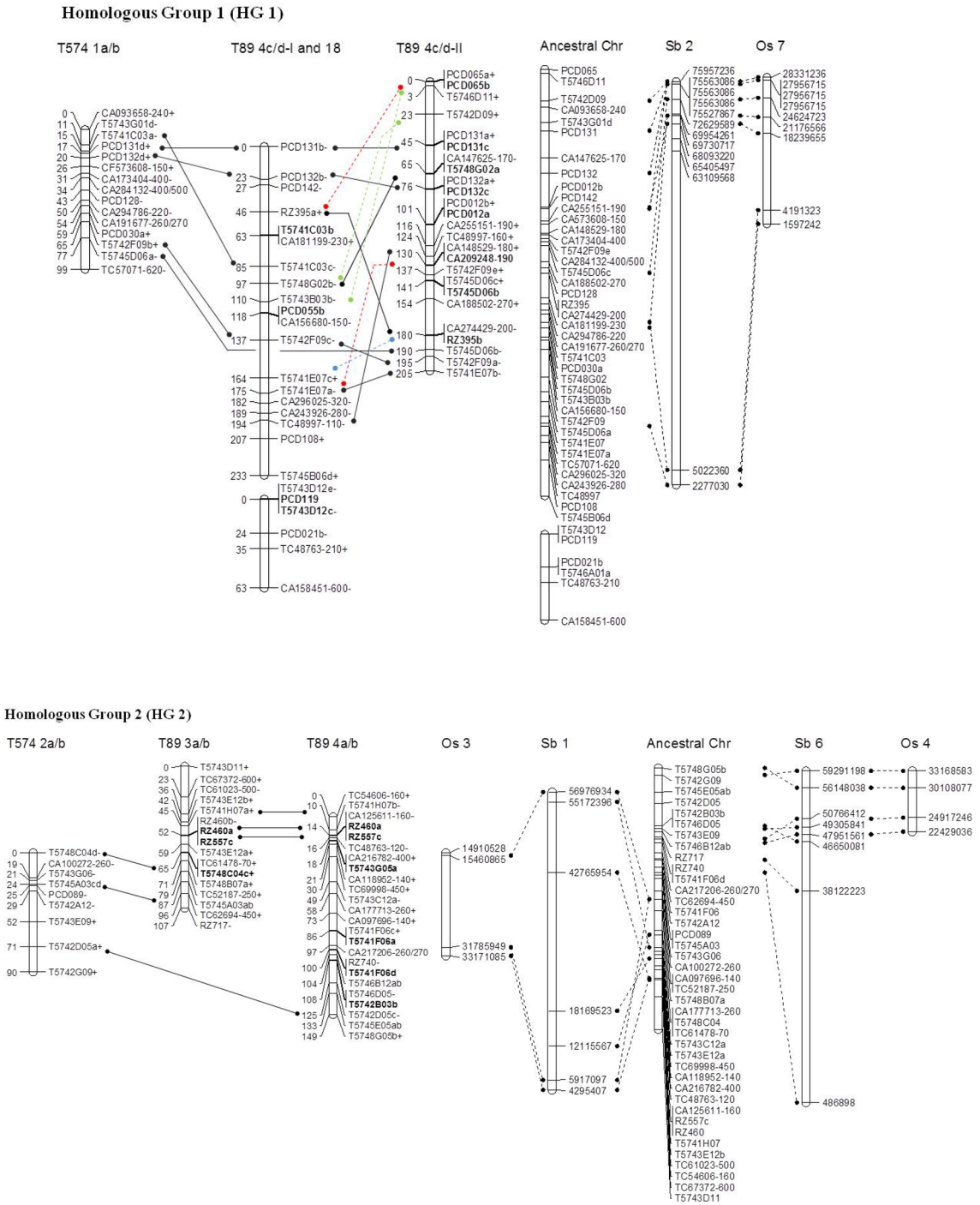

Fig. 1 Linkage maps of *Cynodon* spp., inferred ancestral bermudagrass chromosomes, and homology with *Sorghum* and rice. *Cynodon transvaalensis* ($2x=18$) and *C. dactylon* ($4x=36$) CGs are identified with *T574* and *T89* prefixes, while inferred bermudagrass ancestral chromosomes between the two parents are compared with *Sorghum* (*Sb*) and rice (*Os*) homologs. CA-, CF-, and TC-type markers are sugarcane EST-SSRs. The '±' suffix to mapped markers designates alternative linkage phases. Markers covered by vertical lines map to same locus or in case of a DDM (*bold font*), represents closest linkages. Markers are indicated on the *right*, cumulative distances are on the *left* (in Kosambi cM). T89 map consists of 34 CGs, of which 26 CGs are assigned to one of nine homologous groups. Likewise, 12 of 14 T574 CGs are assigned to homolgous groups. T89 homo(eo) logs are connected with shared multi-locus markers (*solid lines*) and simplex–simplex (*green-dashed* coupling; *red-dashed* repulsion) and simplex-duplex coupling linkages (*blue-dashed lines*). Homologous groups between T574 and T89 are aligned on the basis of multi-locus markers including biparental loci (*solid lines*). *Dashed-solid black lines* connect inferred bermudagrass ancestral chromosomes to putative *Sorghum* and rice homologs

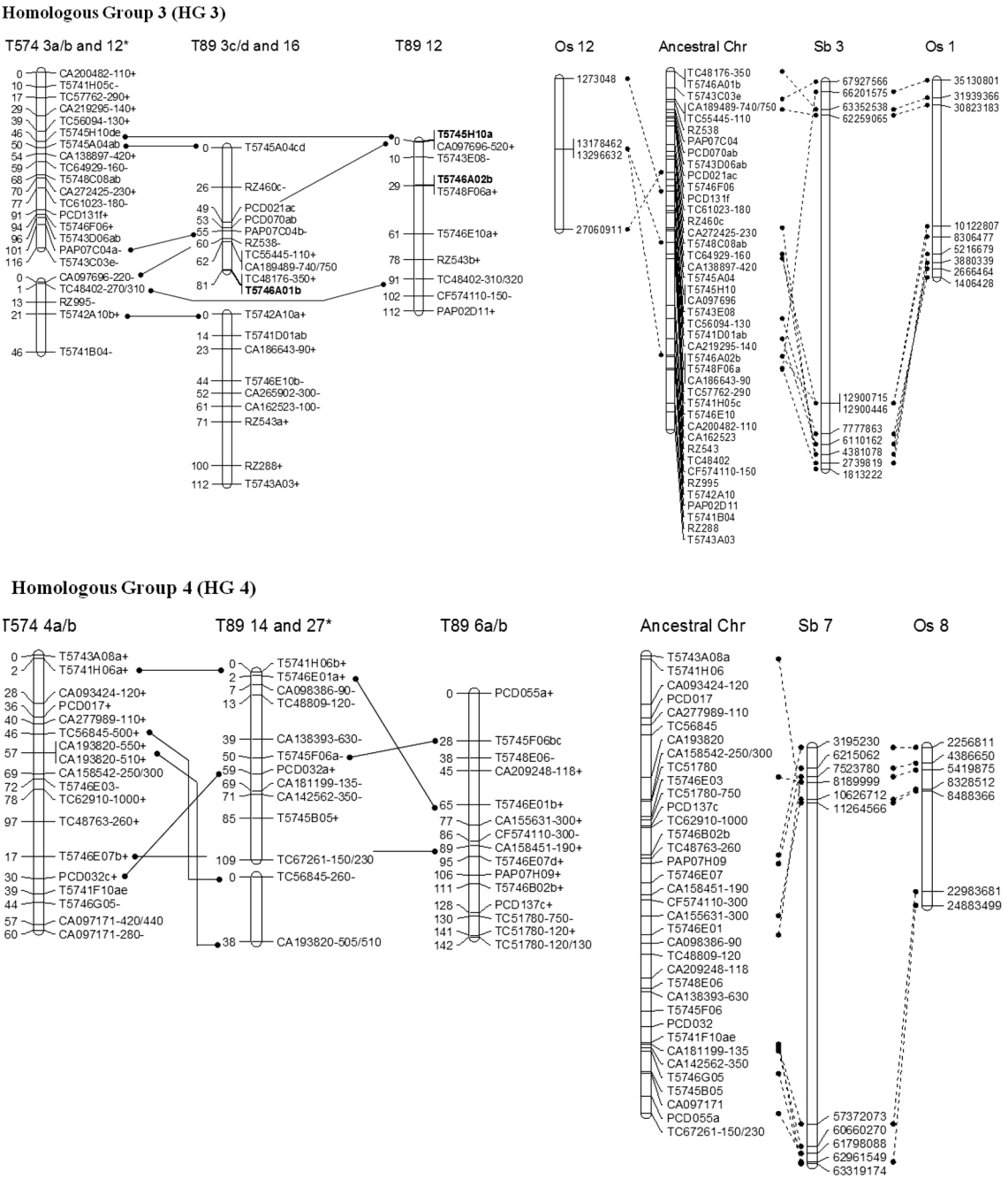

Fig. 1 (continued)

ends of CGs) accounted for 71 and 100% of the increase in map lengths of T89 and T574, respectively. In comparing linkage maps, there were a few noteworthy changes to the current update. LGs T89 1a and T89 1b were split into two CGs, T89 1a/b-I and T89 1a/b-II; and LG T89 4c was also split into two homo(eo)logous CGs, T89 4c-I and T89 4c-II. Similarly, LG complex T574 7a-1, T574 7a-2, and T574 7b was split up into two LGs, namely T574 7a-2/b-I and T574 7a-1/b-II, while T574 8 and T574 10 were merged into one (with the addition of 5 new markers). Further, LG T574 9 exclusively contained coupling linkages in the original framework, but new markers revealed several repulsion linkages.

Superimposition of double-dose markers

Bethel et al. (2006) identified 44 RFLP loci as DDRFs segregating in a 5:1 ratio in the progeny, following Ripol et al.

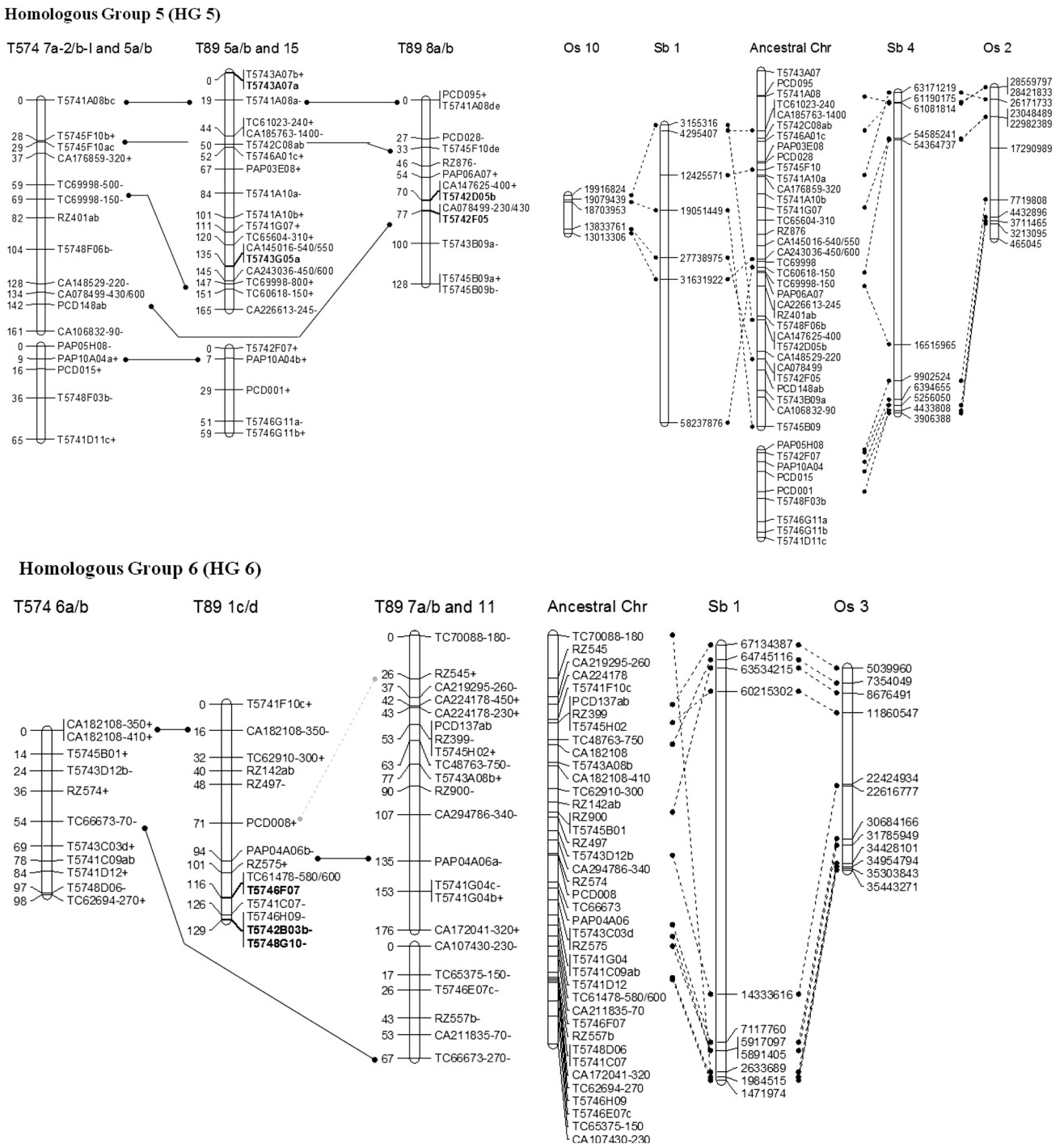

Fig. 1 (continued)

(1999). In contrast to a complete polysomic model tested in Bethel et al. (2006), here all the markers were tested for allelic (i.e. homologous) or non-allelic (i.e., homoeologous or heterologous) duplication that is segregating in ≥3:1 ratio (see "Materials and methods"). A total of 74 loci (i.e., 10 SSRs and 64 RFLPs) were confirmed to have ≥3:1 segregation ratios in the progeny, of which 4 loci were present in T89-duplex by T574-simplex configuration (i.e., segregating in ≥8:1 ratio), respectively.

Out of a total of 70 informative DDMs (i.e., segregating in $3{:}1 \geq x \leq 5{:}1$), 34 (50%) DDMs were involved in a total of 77 significant simplex-duplex linkages ($P = 0.001$). Among these, 54 corresponded to DDMs linked in both coupling and repulsion to SDMs mapped to single CGs,

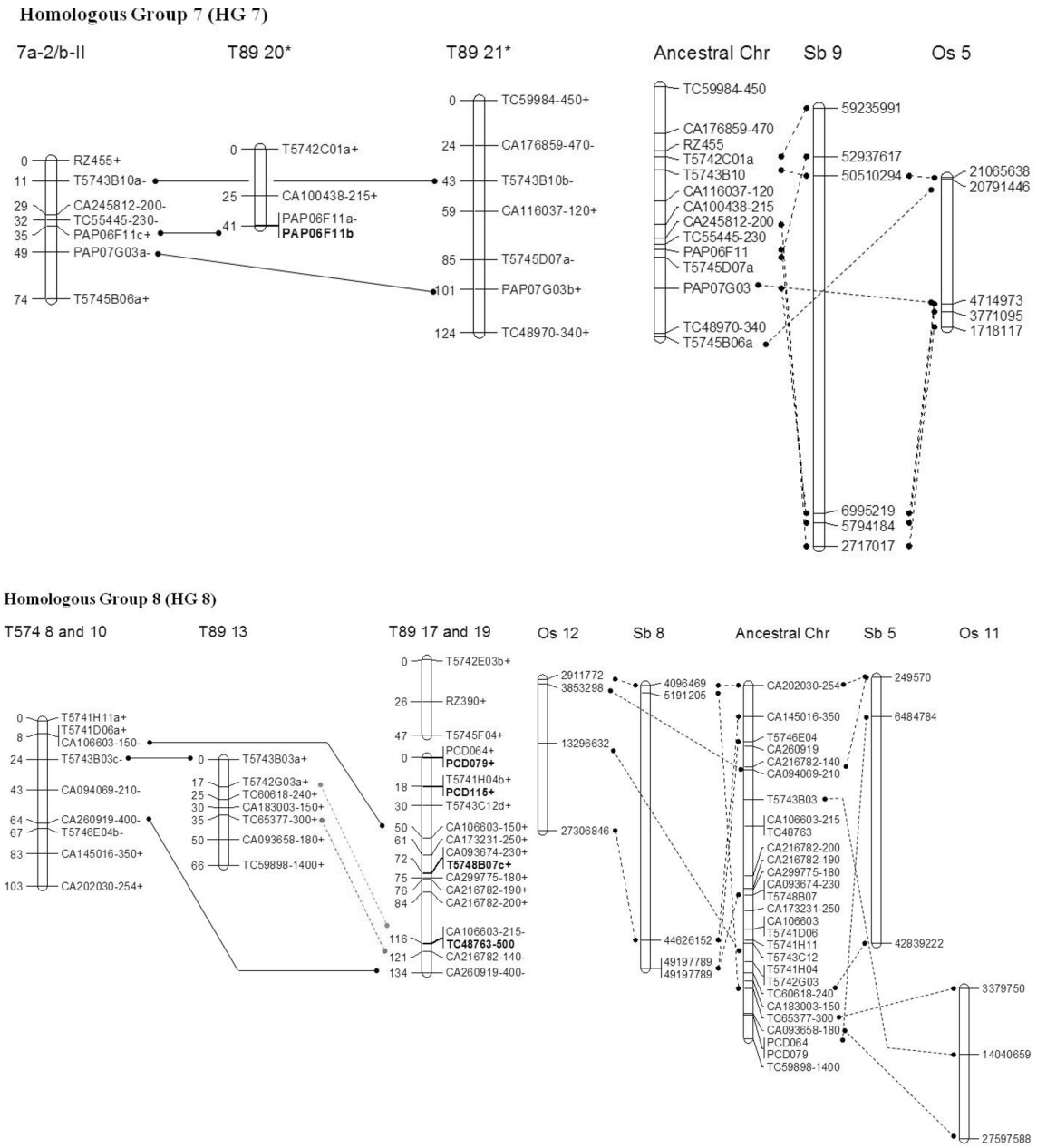

Fig. 1 (continued)

and 10 and 13 simplex–duplex linkages were either in coupling or in repulsion within CGs, respectively. Sixteen additional DDMs showed multiple linkages with simplex markers within CGs, which developed 40 additional linkages, 30 in both coupling and repulsion and 10 only in coupling. Further, eight DDMs were linked in coupling to two different CGs. Of interest, four of the eight markers showed both coupling and repulsion linkages with CGs within assigned homo(eo)logous groups, which satisfies four possible linkages (i.e., two each of coupling and repulsion) that can be detected from a duplex marker. For example, duplex markers RZ460a and RZ557c were significantly linked (in both coupling and in repulsion) to simplex markers in CGs T89 3a/b and T89 4a/b, which formed HG 2 of the integrated map. The remaining four DDMs were linked to CGs associated with different HGs, suggesting heterologous duplications at these loci. Furthermore, two additional DDMs were linked in both coupling and repulsion to single CGs and only in repulsion to its homo(eo)log, leaving one coupling linkage undetected. These include DDMs RZ395b and T5742B11c, which are linked in both coupling and repulsion to T89 4c/d-II and T89 1a/b-I, while linked

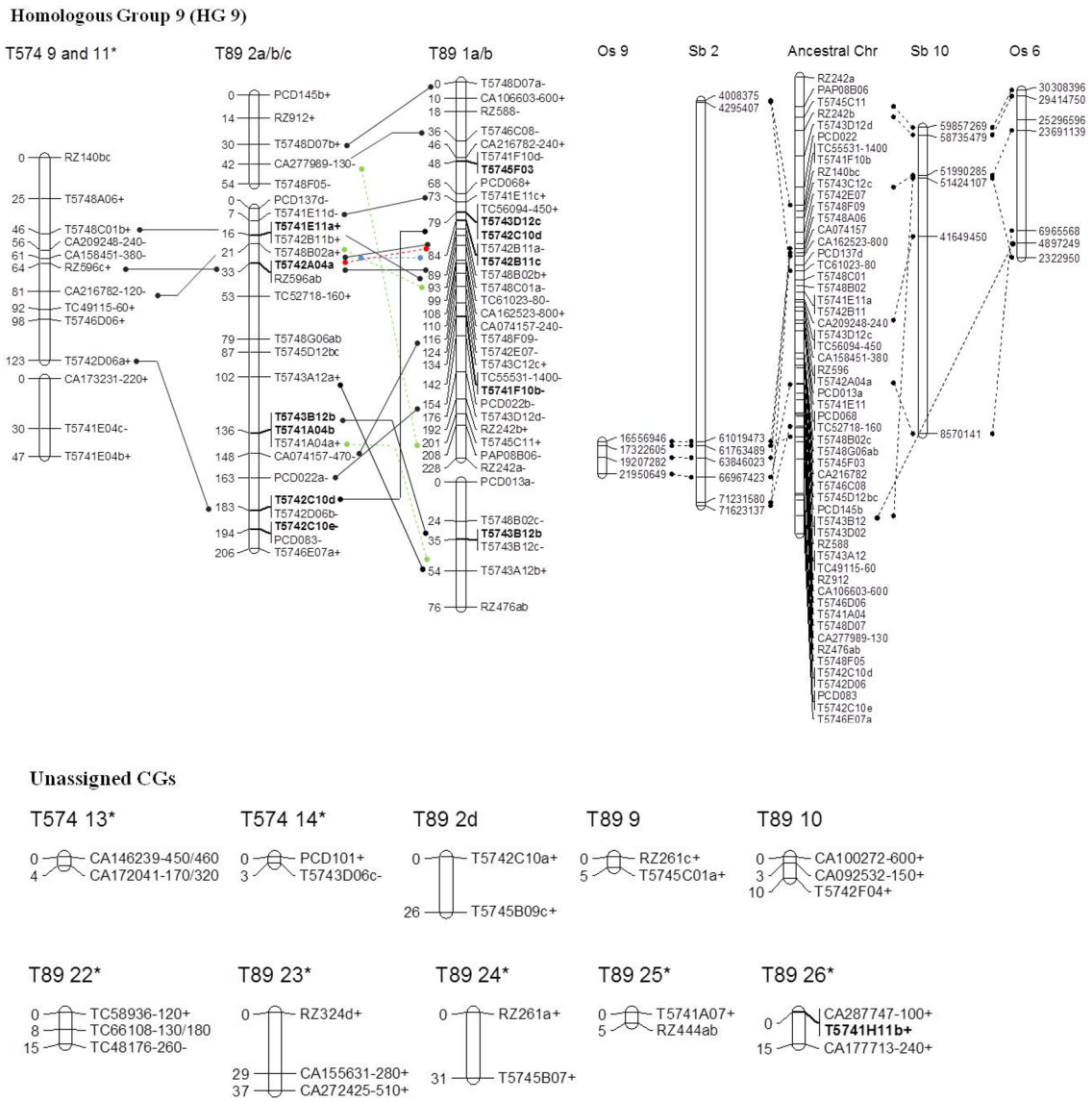

Fig. 1 (continued)

only in repulsion to their homo(eo)logs T89 4c/d-I and T89 2a/b, respectively.

Simplex–duplex associations with at least one significant coupling linkage were super-imposed on the integrated map (Fig. 1), while 13 simplex–duplex repulsion-only linkages were excluded, following Hackett et al. (2007).

Homo(eo)logy assignment of cosegregating groups

The addition of more than 200 loci to the updated map helped to clarify homologous relationships. Originally, four homologous T89 sets were aligned based on shared multilocus probes and repulsion phase linkages (Bethel et al. 2006). For example, consensus 1 of T89 was originally established based on integration of T89 1a, T89 1b, T89 1c, and T89 1d. While several repulsion linkages were detected between T89 1a and T89 1b (i.e., T89 1a/b) and between T89 1c and T89 1d (i.e, T89 1c/d), a single repulsion linkage connected T89 1a/b with T89 1c/d. The specific simplex–simplex repulsion was also detected in this study, but the LOD support was low (<2.5). Further, homo(eo)logy between T89 1a/b, and T89 2a/b/c garnered stronger support to build HG 9 based on 11 shared multilocus markers, 10 simplex–simplex linkages (perhaps displaying residual polysomy), 3 simplex–duplex linkages, and 11 and 14 significant blast hits with rice (i.e., Os 6 and Os 9) and sorghum (i.e., Sb 2 and Sb 10), respectively. Accordingly, nine novel HGs presumed to represent the basic chromosome number of bermudagrass ($x=9$) were built and aligned, all based on strong support from shared multilocus markers,

Table 2 Comparison of T574 and T89 genetic linkage maps of *Cynodon* spp.

	C. transvaalensis (T574)	*C. dactylon* (T89)
Number of cosegregating groups (CGs)	14	34
Total map length (cM)	1188.4	3248.7
Mean length of CG (cM)	84.9	96.0
Largest size of CG (cM)	161.4	233.4
Smallest size of CG (cM)	3.2	4.5
Total number of markers	125	291
RFLP markers	73	178
Codominant	12	18
Dominant	61	160
SSR markers	52	113
Codominant	6	7
Dominant	39	93
Biparental	5	9
Codominant biparental	2	4
Average distance between markers (cM)	10.7	12.5
Marker density (map length/number of markers)	9.5	11.2
Average number of markers per CG	9	8.6
Largest gap size (cM)	29.7	37.8
Number of gaps >30 cM	0	6

significant linkages, and homology with rice and sorghum genomes (Fig. 1).

Estimated recombination lengths and genome coverage

The two methods implemented to estimate genome lengths (see "Materials and methods") from the updated linkage maps assume random distribution of markers in the maps, which were tested using Pearson correlation coefficients. The coefficient values between CG lengths (in cM) and number of markers in T574 and T89 maps were 0.80 and 0.90, respectively, indicating that the marker distributions in both maps are approximately random. Since the two estimates almost coincided, we used their average as expected genome length (Table 3). On the basis of the expected genome length, genome coverage for the T574 and T89 maps is 79.5 and 78.3%, respectively. Considering estimated 1 C genome sizes of *C. transvaalensis* (5.43×10^8 bp) and *C. dactylon* (14.33×10^8) as cataloged in Plant DNA C-values database (http//:data.kew.org/cvalues) following Taliaferro et al. (1997), the present average interval between marker loci is equivalent to 3.9 Mbp in T574 and 4.4 Mbp in T89. Accordingly, 1 cM represents an average of 0.36 Mbp in T574 and 0.35 Mbp in T89. Both maps approach monoploidy once unassigned CGs are excluded. Since two T574 and eight T89 CGs have fewer than 4 markers ($m<4$) and remain unassigned to HGs, they were excluded from marker distribution and genome size and coverage estimates. When only the monoploid maps are taken into consideration, genome coverage increases to 85.8% in T574 and 87.0% in T89, with 4.3 and 5.1 Mbp marker intervals and 0.39 and 0.40 Mbp per cM, respectively. For both maps, ~80% of the genome was within 10 cM of a mapped marker.

Compared to the framework linkage map, updated genome size estimate decreased the T574 map by 73.5 cM

Table 3 Expected and observed map length and genome coverage of *C. transvaalensis* (T574) and *C. dactylon* (T89) genetic maps

	T574	T89	T574 Monoploid-map	T89 Monoploid-map
G_{e1} (cM)	1488.3	4076.5	1373.6	3563.0
G_{e2} (cM)	1502.7	4227.9	1378.4	3578.7
G_e (cM)	1495.5	4152.2	1376.0	3570.8
G_O (cM)	1188.4	3249.6	1181.1	3105.8
Genome coverage (%)	79.5	78.3	85.8	87.0
1 C genome size (Mbp)	543	1433	543	1433
Genome coverage (Mbp)	431	1121	466	1246
Mbp per marker interval	3.9	4.4	4.3	5.1
Mbp per cM	0.36	0.35	0.39	0.40

T574 and T89 monoploid maps; from HG 1 to HG 9. 1 C genome size was obtained from Taliaferro, Hopkins, et al. (1997). *Mbp* mega base pair, G_{e1} estimated length by Fishman et al. (2001), G_{e2} estimated length by Chakravarti et al. (1991), G_e average of G_{e1} and G_{e2}, G_o observed length

and increased the T89 map by 1140.2 cM. However, genome coverage increased by ~17% in both species.

Mode of inheritance in T89

Codominant markers and disomic segregation

A total of 27 T89-specific codominant markers including 8 pairs of SSR and 19 pairs of RFLP alleles were detected, which showed strict disomic segregation at parental heterozygous loci (i.e. 100% complementary presence or absence between the two alleles). Twenty-five codominant markers were associated with 14 different CGs and correspond to 6 HGs, while 2 codominant markers remain unlinked (Fig. 1).

Single dose vs. multiple dose markers

SSR markers showed significant deviations ($P=0.01$) from the expected ratios of 3:1 and 5:1 (single dose vs. multiple dose marker frequencies) for allopolyploid and autopolyploid genome constitution, respectively (Table 4). Dosage ratios for RFLP markers did not deviate significantly from the allopolyploid ratio, while that for overall marker data did not deviate significantly from 5:1 ratio, indicating a much closer correspondence with autopolyploidy.

Frequency of repulsion-phase vs. coupling-phase

A total of 687 coupling and 595 repulsion linkages (LOD ≥ 2, $\theta=0.4$) were detected with averages of 20.2 coupling and 17.5 repulsion per CG (Supplemental Table 2). Although a Chi-squared test determined that the genome-wide ratio of repulsion to coupling linkage was significantly different from a disomic model (i.e. 1:1; $P=0.05$), 20 of 26 CGs did not deviate significantly from the disomic preferential pairing ratio, while eight unassigned CGs with less than 4 markers ($m<4$) were not tested. Furthermore, repulsion linkages were detected across many CGs at linkages of LOD ≥ 4 and $\theta=0.33$, which would be highly unlikely under a completely polysomic model of inheritance (see "Discussion"). The 6 CGs showing significant divergence from the preferential pairing ratio included T89 4c-1/d, and T89 4c-2/d, the homo(eo)logous pair constituting HG 1; T89 CGs constituting HG 8; and T89 11 and T89 6a/b.

Table 4 Summary of Chi-squared tests of simplex to multiplex ratios of T89-associated markers compared to theoretical expectations in allopolyploids and autopolyploids

Marker	Observed (in T89)	Allopolyploid		Autopolyploid	
		Expected	χ^2	Expected	χ^2
SSR					
Simplex	131	105.8	24.11**	117.0	9.81**
Multiplex	10	35.3		24.0	
	141	141		141	
RFLP					
Simplex	211	206.3	0.44 *ns*	228.3	7.67**
Multiplex	64	68.8		46.8	
	275	275		275	
Total					
Simplex	342	312.0	11.54**	345.3	0.18 *ns*
Multiplex	74	104.0		70.7	
	416	416		416	

ns not significant

**Significant at $P=0.01$

Linkages between homo(eo)logous groups

Four homo(eo)logous CG pairs shared linkages within themselves (i.e., markers in putative homoeologs show significant linkages or pseudolinkages) which is suggestive that these homo(eo)logs show incomplete, but random pairing during meiosis (i.e., residual polysomic inheritance). Homo(eo)logous LGs T89 4c/d-I and T89 4c/d-II share seven repulsion and six coupling linkages among 11 simplex markers with average recombination fraction of 0.26 each, supported by average LODs of 3.4 and 2.8, respectively. One significant repulsion phase duplex-simplex linkage was also detected between the two groups. Similarly, homo(eo)logous pair T89 1c/d and T89 7a/b share a coupling linkage (with recombination fraction $r=0.26$ and LOD = 3), while T89 13 and T89 19 share a repulsion linkage (with $r=0.31$ and LOD = 3.3). Further, homo(eo)logous LG pairs T89 2a/b/c and T89 1a/b share six repulsion and four coupling linkages with average recombination fraction of 0.26 and 0.25, respectively, and supported by average LOD of 3.5. Three double-dose markers were also significantly linked to the two LG pairs (T89 2a/b/c and T89 1a/b), supporting the veracity of homo(eo)logy assignment.

Comparative mapping

A bermudagrass ancestral chromosome complement was inferred (see "Materials and methods") and compared with sorghum and rice genomes to identify significant homologies and colinearity (Fig. 1). Five and four of the nine bermudagrass consensus groups corresponded to single homologous chromosomes of sorghum and rice, respectively (Table 5). Each of the remaining four and five inferred consensus groups corresponded to two different chromosomes of sorghum and rice, respectively. Interchromosomal rearrangements were evident in HG 5 and HG 9

Table 5 Number of markers that share high degrees of similarity with sorghum, rice and zoysiagrass pseudomolecules

Homologous group (HG)	Orthologous sorghum chromosome	Significant hits to sorghum genome[a]	Orthologous rice chromosome	Significant hits to rice genome	Orthologous zoysiagrass chromosomes (homoeologs)	Significant hits to zoysiagrass genome [b]
HG 1	Sb 2	13	Os 7	9	Zj 3 and Zj 4	3 and 6 (9)
HG 2	Sb 1 + Sb 6	8 + 7 (15)	Os 3 + Os 4	4 + 4 (8)	Zj 11 and Zj 12	5 and 6 (11)
HG 3	Sb 3	11	Os 1 + Os 12	9 + 5 (14)	Zj 5 + Zj 15 and Zj 6 + Zj 16	7 + 0 and 6 + 0 (13)
HG 4	Sb 7	11	Os 8	7	Zj 13 and Zj 14	3 and 3 (6)
HG 5	Sb 4 + Sb1	11 + 7 (18)	Os 2 + Os 10	11 + 5 (16)	Zj 7 + Zj 1 and Zj 8 + Zj 2	12 + 3 and 12 + 3 (30)
HG 6	Sb 1	11	Os 3	12	Zj 1 and Zj 2	4 and 4 (8)
HG 7	Sb 9	6	Os 5	5	Zj 17 and Zj 18	3 and 3 (6)
HG 8	Sb 5 + Sb 8	3 + 5 (8)	Os 11 + Os 12	3 + 4 (7)	Zj 9 + Zj 15 and Zj 10 + Zj16	0 + 1 and 2 + 1 (4)
HG 9	Sb 10 + Sb 2	6 + 9 (15)	Os 6 + Os 9	7 + 5 (12)	Zj 19 and Zj 20	6 and 6 (12)
Total		108		91		

[a]Numbers in parenthesis are sums of significant hits to different chromosomes

[b]Numbers correspond to significant hits to homoeologous chromosomes and their sums in parenthesis

which involved parts of sorghum chromosomes Sb 2 and Sb 1 relocated into Sb 10 and Sb 4, respectively. These structural rearrangements were also evident when compared to cognate rice homologs and involved nested chromosome fusions (NCFs) between Os 2 and Os 10 and between Os 6 and Os 9.

Inferred ancestral chromosomes were also compared with zoysiagrass pseudomolecules (Tanaka et al. 2016) based on ninety-nine putative homologous sequences (Table 5). Comparative mapping showed that two major NCFs observed in bermudagrass (i.e., in HG 5 and HG 9) were also shared by zoysiagrass. These NCFs were also reported in prior studies in zoysiagrass (Huang et al. 2016; Wang et al. 2015a). Specifically, middle section of Sb 1 nested within Sb 4 in inferred ancestral HG 5 of bermudagrass was consistent with middle section of Sb 1 associated with middle sections of zoysiagrass homologs Zj/Zm 7 and Zj/Zm 8. Similarly, middle section of Sb 2 nested within Sb 10 in inferred ancestral HG 9 was consistent with middle section of Sb 2 corresponding to middle sections of Zj/Zm 19 and Zj/Zm 20. The two NCFs also corroborate with translocation-mediated evolution of finger millet group 2 chromosomes (2A and 2B) and group 6 chromosomes (6A and 6B) as reported (Srinivasachari et al. 2007). Corresponding rearrangements has not been specified in studies concerning other two chloridoids [i.e., tef (Cannarozzi et al. 2014) and prairie cordgrass (Crawford et al. 2016)]. In tef, draft genome assembly was anchored against sorghum pseudomolecules, but a lack of complete and saturated genetic linkage map hindered clear delineation of its karyotype evolution. In prairie cordgrass, genetic markers were anchored to tef scaffolds, which served as a bridge to align its linkage maps to sorghum. Nevertheless, comparative plots reported in tef and prairie cordgrass displayed correspondences relevant to the current study. For example, correspondence chart between tef genetic map (Zeid et al. 2011) and its pseudo-chromosomes apparently traced marker(s) in LG 10 to pseudo-chromosomes 2 and 10 and 11 to 1 and 4 (Cannarozzi et al. 2014). Similarly, prairie cordgrass linkage group 6 corresponded to Sb 1 and Sb 4, while linkage group 4 corresponded to Sb2 and Sb 10. These observations support our assertion that two shared NCFs delineate karyotype evolution in the Chloridoideae subfamily and are distinct from those defining divergent Poales lineages (see "Discussion").

Two additional genome repatterning events were observed in bermudagrass. Several markers in HG 8 showed significant correspondence with Os 11 and Os 12 in the rice genome (corresponding to sorghum Sb 5 and Sb 8). Second, HG 2 showed significant correspondence with both Os 4 and Os 3 (corresponding to Sb 6 and Sb 1), which may represent yet another major reshuffling in the bermudagrass lineage.

Discussion

We report SSR-enriched bermudagrass genetic linkage maps constructed using a full-sib (i.e., F_1) population derived from an interspecific cross between two heterozygous accessions representing tetraploid common bermudagrass (i.e., T89) and diploid African bermudagrass (i.e., T574) as female and male, respectively. Clonal selections from the crosses between these two species have also produced several leading turf varieties, which underscores the importance of investigation into their genomic organization and chromosomal transmission. Further, perenniality and the clonal nature of the mapping population provides

a unique opportunity for QTL analyses across different environments over several years. The information presented in this study establishes a foundation both for basic and applied genetic studies.

The current map adds 207 novel loci to the parental linkage frameworks published earlier (Bethel et al. 2006), which increased genome coverage by ~17% to represent around 85% of the monoploid estimates of both species. In a comparable study, genome coverage with 261 and 303 markers in *Miscanthus* (*M. sacchariflorus* Robustus × *M. sinensis*), was 72.7 and 84.9%, respectively (Kim et al. 2012). Further, the number of SSR polymorphisms that fell on tetraploid chromosomes (i.e., T89) was almost exactly twice that of the diploid (i.e., T574), which is identical to RFLP estimates in Bethel et al. (2006). Therefore, considering more than twofold differences in monoploid length estimates between the diploid and the tetraploid, heterozygosity within T574 and T89 appear comparable.

In the updated parental linkage maps, coupling and repulsion linkages were integrated. However, marker orders did not change substantially relative to the orders in the framework linkage maps (Bethel et al. 2006), supporting correspondence between the results from EM algorithm employed in OneMap (Wu et al. 2002) and the traditional "pseudo-testcross" strategy (Grattapaglia and Sederoff 1994) using MapMaker/EXP (Lander et al. 1987). Since OneMap did not support integrating duplex markers into simplex linkage maps despite established statistical basis (da Silva et al. 1995; Ripol et al. 1999), we used TetraploidMap (Hackett et al. 2007) to detect and verify duplex–simplex linkages. Most duplex–simplex linkages detected and superimposed on the original framework (Bethel et al. 2006) were also verified with TetraploidMap. Fragmented LGs were evident, more so in T89 than T574. Support for some of the fragmented LGs (e.g., HG3 and HG5) was clearly provided by comparative mapping, but more markers are needed to join CGs into complete LGs. For example, CGs of T89 and T574 constituting HG 3 were fragmented, but showed significant BLAST homologies with two different clusters of DNA sequences separated by around 50 Mb in Sb 3 and ~21 Mb in Os 1 (Fig. 1). Since codominant markers are more informative and reliable than random dominant markers (Mollinari et al. 2009; Wu et al. 2003), future mapping efforts will target codominant markers, preferably from bermudagrass sequences homologous to current gaps in coverage of sorghum and rice genomes.

In a pseudo-testcross mapping scheme, biparental markers are necessary to integrate parent-specific linkage maps into a consensus framework (Grattapaglia and Sederoff 1994). In the current study, most SSR markers (84.5% of total) did not deviate significantly from the 1:1 ratio (i.e., presence vs. absence) expected for a single dose segregant in a testcross configuration [i.e., simplex (heterozygous in one parent) by nulliplex (recessive homozygous for null alleles in another parent)], while few SSRs (5.4%) fit the 3:1 ratio (presence vs. absence) expected for a biparental marker in an intercross configuration (i.e., double-simplex or heterozygous in both parents). As such, separate parental linkage maps were constructed due to a paucity of informative bridges. Therefore, more informative markers are needed [i.e., biparental or symmetric (ao × ao) markers] that are closely linked with partially informative ones [(e.g., asymmetric dominant (ao × oo)], where 'a' represents presence of an allele and 'o', a null allele, following (Wu et al. 2002). However, a preponderance of single dose markers and relative paucity of intercross markers are generally expected in interspecific pseudo-testcross mapping. For example, interspecific crosses between *Miscanthus sinensis* × *M. sacchariflorus* (Kim et al. 2012), *Coffea liberica* × *C. eugenioides* (Gartner et al. 2013), and *Poplar adenopoda* × *P. alba* (Yin et al. 2001) each segregated for ~2% of intercross markers. Since the frequency of intercross markers can be significantly improved with intraspecific mapping populations, *C. dactylon* intraspecies maps would provide better opportunities for an integrated map. For example, intraspecific crosses of *Miscanthus sinensis* (Atienza et al. 2002), *Lolium multiflorum* (Hirata et al. 2006), *Fagus sylvatica* (Scalfi et al. 2004), and *Populus deltoides* (Wu et al. 2000), provided 51.5, 36, 15, and 15% of intercross markers, respectively.

Double-dose markers were inferred by a Chi-squared test based on non-significant deviation from ≥3:1 ratios with 99% confidence, which are expected in allelic segregation (i.e., 5:1 ratio between homologous alleles) and non-allelic assortment (i.e., 3:1 ratio between homoeologous or paralogous loci) during tetrasomic (random chromosome pairing) and disomic (preferential chromosome pairing) inheritance, respectively. Interestingly, 17 T574 markers also fit ≥3:1 ratios, 7 of which were associated with CGs T574 1a/b and 3a/b. Presence of double-dose markers in diploid *C. transvaalensis* may come from illegitimate recombination, suggested by the observation of Forbes and Burton (1963) of irregular meiosis in some accessions of the species. We note that these chromosomes do not appear to be ancient homoeologs.

Mode of inheritance

Polyploidy creates evolutionary novelty (Soltis et al. 2014). The ubiquity of polyploid species in higher plant taxa and their recurrent origins assert to their evolutionarily success (Soltis and Soltis 1999). The age and degree of homology between subgenomes of a polyploid influences its chromosomal pairing behavior at meiosis, which dictates its mode of inheritance (i.e., disomic or polysomic). Polysomic inheritance through random chromosome pairing

is associated with autopolyploidy (duplication of a single genome), while disomic inheritance through preferential chromosome pairing is associated with allopolyploidy (merger of divergent genomes in a common nucleus by interspecific hybridization). In autopolyploids, 'diploidization', comprising divergence of homologous sequences and chromosomes by a variety of mechanisms, leads to a shift from random to preferential chromosome pairing; consequently, an autopolyploid may eventually become a diploid species (DeWet 1980; Le Comber et al. 2010). As such, species of autopolyploid origin may display random pairing among some homologs and preferential pairing among others during meiosis (Lentz et al. 1983; Matsubayashi 1991; Sybenga 1994), leading to a mosaic of disomic and polysomic inheritance at different loci, and making it difficult to unambiguously determine genome constitution (Stebbins 1947).

In the current study, we assessed different lines of evidence regarding the type of polyploidy in tetraploid bermudagrass, for which long standing classification as an autopolyploid (Harlan et al. 1966; Hoff 1968) has recently been challenged (Gong et al. 2013; Guo et al. 2015; Harris-Shultz et al. 2010a). Cytological studies in tetraploid accessions of common bermudagrass frequently report multivalents (Forbes and Burton 1963; Hanna and Burton 1977; Hoff 1968), which may suggest autopolyploid genome constitution of the cosmopolitan species (Muntzing 1936). However, a low frequency of multivalents and possibility of subgenome differentiation in tetraploid *C. dactylon* may either indicate segmental allopolyploidy or almost complete diploidization following its autopolyploid origin (Brilman 1981). Fluorescence *in situ* hybridization and meiotic study by Gong et al. (2013) further reinforces the notion. Notably, the proposed genome constitution of tetraploid bermudagrass has not been revisited and unequivocally reviewed. Nevertheless, the occurrence of a high frequency of functional unreduced gametes (Harlan and de Wet 1969) and presence of both diploid and tetraploid chromosome races in at least three different *Cynodon* species (de Wet and Harlan 1970) provide a cytological basis for autopolyploid origin of tetraploid accessions. Further, a single extant diploid species (i.e., *C dactylon* var. *aridus*) shares similar morphological features with common bermudagrass (i.e., *C. dactylon* var. dactylon), including the presence of rhizomes, and displays cross compatibility and sympatric distribution with the latter, suggesting that the diploid species is the only likely source of the tetraploid accession (Harlan and de Wet 1969; Wu 2011). However, the current state of ploidy cannot be unambiguously ascertained solely based on cytotaxonomic and/or morphotaxonomic studies.

Bethel et al. (2006), Harris-Shultz et al. (2010a), and Guo et al. (2015) have used molecular markers to decipher the genome constitution of common bermudagrass. In this study, detection of 25 pairs of T89-specific alleles showing disomic inheritance in the segregating progenies suggest preferential pairing among 14 CGs carrying those alleles. Harris-Shultz et al. (2010a) also found 14 codominant EST-SSRs showing disomic inheritance in the same population. The results are also consistent with Guo et al. (2015), in which 13 of 32 codominant SSRs did not deviate significantly from the 1:2:1 ratio ($P=0.01$) expected in selfed progenies (S1) of a heterozygous individual. These studies all indicate subgenome differentiation, strong preferential pairing, and disomic inheritance attributes which would suggest allopolyploidy as the current state of genome constitution in common bermudagrass. However, marker profiles for 18 primer pairs in Guo et al. (2015) did not fit either disomic or polysomic inheritance ratios (although smaller χ^2 values were associated with disomic ratios), while one locus did not deviate significantly from either (as tested by the authors). Similarly, akin to three genotypes showing uncharacteristic segregation patterns in this study (see "Results"), Harris-Shultz et al. (2010a) also found one aberrant genotype with null alleles at a codominant locus, which could be because of meiotic aberration [as frequently reported in tetraploid accessions (Forbes and Burton 1963; Hanna and Burton 1977; Hoff et al. 1968)] or incomplete preferential pairing (i.e., a characteristic of a segmental polyploid). Further, three homo(eo)logous pairs in our study lacked codominant markers and displayed partial polysomic inheritance (further discussed below). As such, common bermudagrass apparently shows mixed inheritance, a hypothesis that may be further supported by the fact that the ratio of simplex to multiplex markers for RFLPs did not deviate significantly from the disomic ratio, while that for overall marker data fit polysomic expectations. However, different marker systems (i.e., RFLPs and SSRs) may show different levels of subgenome differentiation, with SSRs being well known to evolve new alleles relatively rapidly. Accordingly, ratios of simplex to multiplex markers could be characteristically different between the two marker systems and warrant further investigation.

Comparable numbers of markers in repulsion and coupling linkages for 20 of 26 testable co-segregating groups suggest that most basic *Cynodon* chromosomes pair preferentially. Further, the majority of significant repulsion linkages were detected at $\theta=0.33$, which would be unlikely under a complete polysomic model of inheritance. Even completely linked markers in repulsion phase (i.e., $Rc=0$, where Rc is recombination fraction due to crossing-over) would show a recombination fraction of 0.33 due to independent assortment alone (i.e., $Ri=0.33$, where Ri recombination fraction resulting from independent assortment) (Qu and Hancock 2001). In fact, repulsion linkages associated with six CGs that did not fit the disomic model of

inheritance were also detected at $\theta = 0.33$, which would strongly suggest partial preferential association rather than completely random homologous pairing during meiosis. Further, four of these six CGs were also associated with two homo(eo)logous pairs that share linkages. In particular, homo(eo)logs T89 4c/d-I and T89 4c/d-II shared 13 and 1 significant simplex–simplex and simplex–duplex linkages, respectively, while homo(eo)logs T89 13 and T89 19 shared a repulsion phase marker. These lines of evidence together with a lack of codominant markers suggest that these homo(eo)logous groups exhibit partial polysomic inheritance. In the past, unequivocal cases of segmental polyploidy were lacking (Sybenga 1996), but recently, cases of residual polysomy and/or intermediate inheritance have been reported in several plant species including octoploid strawberry (Rousseau-Gueutin et al. 2008) and garden dahlias (Schie et al. 2014), hexaploid chrysanthemum (Linde et al. 2014) and *Pennisetum*, tetraploid buffelgrass (Jessup et al. 2003) and yellow cress (Stift et al. 2008).

Based on the results of the current studies and long standing evidence that tetraploid bermudagrass has an autopolyploid origin, we conclude that it is in a relatively advanced state of diploidization, behaving as a segmental polyploid. As Wu et al. (1992) put it in their seminal paper: "polyploidy is a state, not a process or an event". Tetraploid bermudagrass appears to represent a species in the process of transitioning to a diploid state. The transition is further evident from the facts that very few multilocus markers mapped to the homo(eo)logous CGs and that several homo(eo)logous pairs showed rearrangements. Further, while almost twice as many polymorphisms occurred in T89 than T574, ploidy-independent frequency of amplicons was observed between the two parental accessions (our unpublished data), indicating that primer pairs predominantly amplified only one of the two homo(eo)logous loci in T89. These lines of evidence strongly suggest substantial subgenome differentiation in common bermudagrass, which is further supported by Guo et al. (2015), where only one primer pair (out of thirty-three) potentially amplified homo(eo)logous amplicons. Also, organellar and nuclear DNA evidence suggested post-WGD rapid diversification of polyploid bermudagrass (Gulsen et al. 2009; Gulsen 2011). However, high-density genetic linkage maps, preferably using third-generation marker systems (i.e., genotyping-by-sequencing), are warranted to clearly delineate subgenome differentiation in common bermudagrass.

Genome evolution in chloridoid lineages

Grasses evolved from a base ancestral karyotype of $n = 7$ that subsequently underwent WGD ($n = 14$) followed by two chromosome fusions (CFs) to attain an intermediate ancestral karyotype of $n = 12$, which among extant grasses is best represented by the modern rice ($n = 12$) genome (Wang et al. 2015b). Comparative analysis indicated one-to-one and one-to-two correspondence between bermudagrass inferred ancestral chromosomes and cognate sorghum and rice chromosomes (Table 5). General conservation of synteny and colinearity was evident between bermudagrass and the two model genomes, with few large-scale chromosomal rearrangements. Two NCFs in bermudagrass (i.e., in HG 5 and HG 9) were also detected in zoysiagrass ($n = 10$) (Table 5) (Huang et al. 2016; Wang et al. 2015a) and finger millet ($n = 9$) (Srinivasachari et al. 2007), while tef and prairie cordgrass genomes also apparently share these rearrangements (see "Results"), which implicates these NCFs in the 14-to-10 chromosomal reduction process in chloridoid lineages. Therefore, they may represent major genome restructuring, perhaps in a single step, in the common ancestral chloridoid. Evidently, these NCFs are different from those that occurred in sorghum and foxtail millet (Murat et al. 2010; Wang et al. 2015b). Furthermore, bermudagrass and finger millet underwent additional genome reshuffling that conferred their basal chromosome number of 9. Two additional genome repatterning events were evident in bermudagrass, which were both different from the third NCF event in the finger millet lineage involving Sb 8 and Sb 9 (corresponding to Os 12 and Os 5) (Srinivasachari et al. 2007). Instead, the third probable NCF event in bermudagrass may involve a merger between paleo-homoeologous chromosomes Sb 5 and Sb 8 (corresponding to Os 11 and Os 12), to constitute HG 8. Akin to *Brachypodium* in which three of 7 NCF events involved ancestral duplications (Wang et al. 2015b), bermudagrass HG 8 may represent a fusion between the two pan-cereal paleo-homoeologs.

Similarly, HG 2 showed significant homology with Sb 6 and Sb 1 (corresponding to Os 4 and Os 3), which may represent yet another major reshuffling in the bermudagrass lineage (a hypothesis that needs further assessment). Although the tef genome would provide additional support for comparative analysis in chloridoid species, lack of complete and saturated linkage maps curtailed the possibility of aligning its pseudo-chromosomes to its linkage maps to adequately delineate its chromosomal rearrangements (Cannarozzi et al. 2014). A tef-specific translocation between Sb 3 and Sb 9 (Cannarozzi et al. 2014) was evidently not shared by zoysiagrass (Huang et al. 2016; Tanaka et al. 2016; Wang et al. 2015b), finger millet (Srinivasachari et al. 2007) or bermudagrass (current study), suggesting species-specific rearrangement. Although the current study did not permit large scale comparative analysis to make unequivocal assertions about bermudagrass genome evolution, it demonstrates the feasibility of comparative genomics to navigate inadequately charted genomic landscapes of the chloridoids.

Conclusion

In the current study, a framework linkage map of the bermudagrass genome based on an interspecific cross (*C. dactylon* × *transvaalensis*) was substantially enriched, providing new insight into chloridoid transmission and evolutionary genetics. Common bermudagrass primarily showed disomic inheritance with irrefutable hints of residual polysomic inheritance, indicating that its current genome constitution is a segmental allopolyploid. The updated map is suitable for exploratory QTL analysis since ~80% of the genome lies within 10 cM of a mapped marker. Accordingly, we are currently investigating marker-trait associations for a number of qualitative and quantitative traits relevant to the bermudagrass industry, particularly turf. Basic and applied genetic research in bermudagrass is expected to broaden understanding of evolutionary, structural, and functional genomics of plants.

Author contribution statement SK was responsible for designing and performing the experiments, data analysis and manuscript writing as a part of his PhD research. CK helped in marker screening and reviewed data analysis. SAA, LKR and JA performed experiments. BS served as SK's PhD committee member, maintained the mapping population, and provided feedback on the proposed work and manuscript before submission. AHP conceived the project, oversaw development and initial analysis of the framework map, served as SK's major advisor and revised the manuscript before submission.

Acknowledgements This work was financially supported by the United States Golf Association (USGA), Georgia Seed Development Commission, Georgia Crop Improvement Association, and Georgia Agricultural Experiment Station.

Compliance with ethical standards

Conflict of interest The authors declare that they have no conflict of interest.

References

Altschul SF, Madden TL, Schaffer AA, Zhang J, Zhang Z, Miller W, Lipman DJ (1997) Gapped BLAST and PSI-BLAST: a new generation of protein database search programs. Nucl Acids Res 25(17):3389–3402

Atienza S, Satovic Z, Petersen K, Dolstra O, Martín A (2002) Preliminary genetic linkage map of *Miscanthus sinensis* with RAPD markers. Theor Appl Genet 105:946–952

Bartholomé J, Mabiala A, Savelli B, Bert D, Brendel O, Plomion C, Gion J-M (2015a) Genetic architecture of carbon isotope composition and growth in *Eucalyptus* across multiple environments. New Phytol 206:1437–1449

Bartholomé J, Mandrou E, Mabiala A, Jenkins J, Nabihoudine I, Klopp C, Schmutz J, Plomion C, Gion J-M (2015b) High-resolution genetic maps of *Eucalyptus* improve *Eucalyptus grandis* genome assembly. New Phytol 206:1283–1296

Bassam BJ, Caetano-Anolles G, Gresshoff PM (1991) Fast and sensitive silver staining of DNA in polyacrylamide gels. Anal Biochem 196:80–83

Bethel CM, Sciara EB, Estill JC, Bowers JE, Hanna W, Paterson AH (2006) A framework linkage map of bermudagrass (*Cynodon dactylon* × *transvaalensis*) based on single-dose restriction fragments. Theor Appl Genet 112:727–737

Brilman LAM (1981) Chromosome morphology in *Cynodon dactylon* (L.) Pers. Dissertation Abstracts International, B, pp 3968B–3968B

Burton GW (1960) Tifway bermudagrass. US Golf Ass J 13:28–30

Burton GW, Hart RH (1967) Use of self-incompatibility to produce commercial seed-propagated F_1 bermudagrass hybrids. Crop Sci 7:524–527

Cannarozzi G, Plaza-W ü thrich S, Esfeld K, Larti S, Wilson YS, Girma D, Castro E, Chanyalew S, Bl ö sch R, Farinelli L, Lyons E, Schneider M, Falquet L, Kuhlemeier C, Assefa K, Tadele Z (2014) Genome and transcriptome sequencing identifies breeding targets in the orphan crop tef (Eragrostis tef). BMC Genom 15:581. doi:10.1186/1471-2164-15-581

Cerda ER, Aldaco Nuncio RA, Montemayor Trejo JA, Hernández MF, Ramírez JO, Villagómez Gamboa JC (2007) Exploitation and improvement of saline soils through the establishment of forage grasses. Técnica Pecuaria en México 45:19–24

Chakravarti A, Lasher LK, Reefer JE (1991) A maximum likelihood method for estimating genome length using genetic linkage data. Genetics 128:175–182

Chittenden LM, Wing RA, Paterson AH, Wing RA, Schertz KF, Lin YR (1994) A detailed RFLP map of *Sorghum bicolor* × *S. propinquum*, suitable for high-density mapping, suggests ancestral duplication of *Sorghum* chromosomes or chromosomal segments. Theor Appl Genet 87:925–933

Crawford J, Brown PJ, Voigt T, Lee DK (2016) Linkage mapping in prairie cordgrass (*Spartina pectinata* Link) using genotyping-by-sequencing. Mol Breed 36:62. doi:10.1007/s11032-016-0484-9

Da Silva J, Honeycutt R, Burnquist W, Al-Janabi S, Sorrells M, Tanksley S, Sobral BS (1995) *Saccharum spontaneum* L. 'SES 208' genetic linkage map combining RFLP- and PCR-based markers. Mol Breed 1:165–179

De Wet JMJ (1980) Origins of polyploids. In: Lewis WH (ed) Polyploidy: biological relevance Part I polyploidy and plant evolution. Plenum Press, New York, pp 3–15

De Wet JMJ, Harlan JR (1970) Biosystematics of *Cynodon* L. C. Rich. (Gramineae). International Bureau for Plant Taxonomy and Nomenclature, pp 565

Dempster AP, Laird NM, Rubin DB (1977) Maximum Likelihood from incomplete data via the EM algorithm. R Stat Soc 1

Elekes CC, Dumitriu I, Busuioc G, Iliescu NS (2010) The appreciation of mineral element accumulation level in some herbaceous plants species by ICP–AES method. Environ Sci Pollut Res 17:1230–1236

Fierst JL (2015) Using linkage maps to correct and scaffold *de novo* genome assemblies: methods, challenges, and computational tools. Front Genet 6:220

Fishman L, Kelly AJ, Morgan E, Willis JH (2001) A genetic map in the *Mimulus guttatus* species complex reveals transmission ratio distortion due to heterospecific interactions. Genetics 159:1701–1716

Forbes IJ, Burton GW (1963) Chromosome numbers and meiosis in some *Cynodon* species and hybrids. Crop Sci 3:75–79

Garcia AAF, Kido EA, Meza AN, Souza HMB, Pinto LR, Pastina MM, Leite CS, Silva JAGd, Ulian EC, Figueira A, Souza AP (2006) Development of an integrated genetic map of a sugarcane (*Saccharum* spp.) commercial cross, based on a maximum-likelihood approach for estimation of linkage and linkage phases. Theor Appl Genet 112:298–314

Gartner G, McCouch S, Moncada M (2013) A genetic map of an interspecific diploid pseudo testcross population of coffee. Euphytica 192:305–323

Gong Z, Xue C, Zhang M, Wang M (2013) Distribution of rDNA loci and genome differentiation in tetraploid *Cynodon*. Indian J Genet Plant Breed 73:459–461

Grattapaglia D, Sederoff R (1994) Genetic linkage maps of *Eucalyptus grandis* and *Eucalyptus urophylla* using a pseudo-testcross: mapping strategy and RAPD markers. Genetics 137:1121–1137

Gulsen OCA (2011) Elucidating polyploidization of bermudagrasses as assessed by organelle and nuclear DNA markers. OMICS 15:903–912

Gulsen O, Sever-Mutlu S, Mutlu N, Tuna M, Karaguzel O, Shearman RC, Riordan TP, Heng-Moss TM (2009) Polyploidy creates higher diversity among *Cynodon* accessions as assessed by molecular markers. Theor Appl Genet 118:1309–1319

Guo Y, Wu Y, Anderson JA, Moss JQ, Zhu L (2015) Disomic inheritance and segregation distortion of SSR markers in two populations of *Cynodon dactylon* (L.) Pers. var. *dactylon*. PLoS One 10:1–10

Hackett CA, Luo Z, Bradshaw JE, Milne I (2007) TetraploidMap for windows: linkage map construction and QTL Mapping in autotetraploid species. J Heredity 98:727–729

Hanna W, Burton GW (1977) Cytology and fertility of some hybrid bermudagrass cultivars. Crop Sci 17:243–245

Harlan JR (1970) Cynodon species and their value for grazing and hay. Herbage Abstr 40:233–238

Harlan JR, de Wet JMJ (1969) Sources of variation in *Cynodon dactylon* (L.) Pers. Crop Sci 9:774–778

Harlan JR, de Wet JMJ, Richardson WR, Huffine WW, Deakin J (1966) Bio-systematics of the genus *Cynodon* (Gramineae). A report of progress, 1965. Proc Ser P-537 Okla agric Exp Stn, pp 34–34

Harlan JR, et al. (1970) A guide to the species of *Cynodon* (Gramineae). Bull Okla Agric Exp Stn B-673:37–37

Harris KR, Schwartz BM, Paterson AH, Brady JA (2010b) Identification and mapping of nucleotide binding site-leucine-rich repeat resistance gene analogs in bermudagrass. J Am Soc Hortic Sci 135:74–82

Harris-Shultz KR, Schwartz BM, Brady JA (2011) Identification of simple sequence repeat markers that differentiate bermudagrass cultivars derived from 'Tifgreen'. J Am Soc Hortic Sci 136:211–218

Harris-Shultz KR, Schwartz BM, Hanna WW, Brady JA (2010a) Development, linkage mapping, and use of microsatellites in bermudagrass. J Am Soc Hortic Sci 135:511–520

Hein MA (1961) Registration of varieties and strains of bermudagrass, III. [*Cynodon dactylon* (L.) Pers.]. Agron J 53:276–276

Hirata M, Komatsu T, Takamizo T, Fujimori M, Miura Y, Cai H, Inoue M, Yuyama N (2006) Development of simple sequence repeat (SSR) markers and construction of an SSR-based linkage map in Italian ryegrass (*Lolium multiflorum* Lam.). Theor Appl Genet 113:270–279

Hoff BJ (1968) The cytology and fertility of bermudagrass, (*Cynodon dactylon* L.) Pers., in Arizona. Dissertation Abstracts, pp 2227B–2227B

Huang X, Wang F, Singh R, Reinert JA, Engelke MC, Genovesi AD, Chandra A, Yu Qingyi (2016) Construction of high-resolution genetic maps of *Zoysia matrella* (L.) Merrill and applications to comparative genomic analysis and QTL mapping of resistance to fall armyworm. BMC Genom 17(1):562

Jessup RW, Burson BL, Burow O, Wang YW, Chang C, Li Z, Paterson AH, Hussey MA (2003) Segmental allotetraploidy and allelic interactions in buffelgrass (*Pennisetum ciliare* (L.) Link syn. *Cenchrus ciliaris* L.) as revealed by genome mapping. Genome / National Research Council Canada = Génome / Conseil National De Recherches Canada 46:304–313

Kawahara Y, de la Bastide M, Hamilton J, Kanamori H, McCombie W, Ouyang S, Schwartz D, Tanaka T, Wu J, Zhou S, Childs K, Davidson R, Lin H, Quesada-Ocampo L, Vaillancourt B, Sakai H, Lee S, Kim J, Numa H, Itoh T, Buell C, Matsumoto T (2013) Improvement of the *Oryza sativa* Nipponbare reference genome using next generation sequence and optical map data. Rice 6:1

Kamps TL, Williams NR, Ortega VM, Chamusco KC, Harris-Shultz K, Scully BT, Chase CD (2011) DNA polymorphisms at bermudagrass microsatellite loci and their use in genotype fingerprinting. Crop Sci 51:1122–1131

Kang S, Lee G, Lim K, Lee H, Park I, Chung S, Kim J, Kim D, Rhee H (2008) Genetic diversity among Korean bermudagrass (*Cynodon* spp.) ecotypes characterized by morphological, cytological and molecular approaches. Mol Cells 25:163–171

Kim CS, Jang CS, Kamps TL, Robertson JS, Feltus FA, Paterson AH (2008) Transcriptome analysis of leaf tissue from Bermudagrass (*Cynodon dactylon*) using a normalised cDNA library. Funct Plant Biol 35:585–594

Kim C, Tang H, Paterson AH (2009) Duplication and divergence of grass genomes: integrating the chloridoids. Trop Plant Biol 2:51–62

Kim C, Zhang D, Auckland SA, Rainville LK, Jakob K, Kronmiller B, Sacks EJ, Deuter M, Paterson AH (2012) - SSR-based genetic maps of *Miscanthus sinensis* and *M. sacchariflorus*, and their comparison to sorghum. Theor Appl Genet 124:1325–1338

Kosambi DD (1944) The estimation of map distances from recombination values. Ann Eugen 12:172–175

Lander ES, Green P, Abrahamson J, Barlow A, Daly MJ, Lincoln SE, Newburg L (1987) MAPMAKER: an interactive computer package for constructing primary genetic linkage maps of experimental and natural populations. Genomics 1:174–181

Lange K (1982) How many polymorphic genes will it take to span the human genome? Am J Hum Genet 34:842–845

Le Comber SC, Ainouche ML, Kovarik A, Leitch AR (2010) Making a functional diploid: from polysomic to disomic inheritance. Blackwell Publishing, p 113

Lentz EM, Loegering WQ, Sleper DA, Crane CF (1983) An assessment of preferential chromosome pairing at meiosis in *Dactylis glomerata*. Can J Genet Cytol. Journal canadien de genetique et de cytologie 25:222–232

Linde M, Debener T, Klie M, Schie S (2014) The type of ploidy of chrysanthemum is not black or white: a comparison of a molecular approach to published cytological methods. Front Plant Sci 5:1–8

Ling Y, Zhang XQ, Ma X, Chen SY, Chen TT, Liu W (2012) Analysis of genetic diversity among wild bermudagrass germplasm from southwest China using SSR markers. Genet Mol Res GMR 11:4598–4608

Lowry D, Taylor S, Bonnette J, Aspinwall M, Asmus A, Keitt T, Tobias C, Juenger T (2015) QTLs for biomass and developmental traits in switchgrass (*Panicum virgatum*). Bioenerg Res 1–12

Margarido GRA, Souza AP, Garcia AAF (2007) OneMap: software for genetic mapping in outcrossing species. Hereditas 144:78–79

Matsubayashi M (1991) Phylogenetic relationships in the potato and its related species. In: Tsuchiya T, Gupta PK (eds) Chromosome

engineering in plants: genetics, breeding, evolution Part B. Elsevier Science Publishers, Amsterdam
Mollinari M, Margarido GRA, Vencovsky R, Garcia AAF (2009) Evaluation of algorithms used to order markers on genetic maps. Heredity 103:494–502
Muntzing A (1936) The evolutionary significance of autopolyploidy. Hereditas 21:263–378
Murat F, Xu JH, Tannier E, Abrouk M, Guilhot N, Pont C, Messing J, Salse J (2010) Ancestral grass karyotype reconstruction unravels new mechanisms of genome shuffling as a source of plant evolution. Genome Res 20(11):1545–1557
Oliveira KM, Pinto LR, Marconi TG, Margarido GRA, Pastina MM, Teixeira LHM, Figueira AV, Ulian EC, Garcia AF, Souza AP (2007) Functional integrated genetic linkage map based on EST-markers for a sugarcane (*Saccharum* spp.) commercial cross. Mol Breed 20:189–208
Oliveira EJ, Vieira MLC, Garcia AAF, Munhoz CF, Margarido GRA, Consoli L, Matta FP, Moraes MC, Zucchi MI, Fungaro MHP (2008) An integrated molecular map of yellow passion fruit based on simultaneous maximum-likelihood estimation of linkage and linkage phases. J Am Soc Hortic Sci 133:35–41
Palhares AC, Rodrigues-Morais TB, Sluys MAv, Domingues DS, Maccheroni W, Jordão H, Souza AP, Marconi TG, Mollinari M, Gazaffi R, Garcia AAF, Vieira MLC (2012) A novel linkage map of sugarcane with evidence for clustering of retrotransposon-based markers. BMC Genet 13:51. doi:10.1186/1471-2156-13-51
Paterson AH, Bowers JE, Bruggmann R, Dubchak I, Grimwood J, Gundlach H, Haberer G, Hellsten U, Mitros T, Poliakov A, Schmutz J, Spannagl M, Tang H, Wang X, Wicker T, Bharti AK, Chapman J, Feltus FA, Gowik U, Grigoriev IV (2009) The *Sorghum bicolor* genome and the diversification of grasses. Nature 457:551–556
Pereira GS, Nunes ES, Laperuta LDC, Braga MF, Penha HA, Diniz AL, Munhoz CF, Gazaffi R, Garcia AAF, Vieira MLC (2013) Molecular polymorphism and linkage analysis in sweet passion fruit, an outcrossing species. Ann Appl Biol 162:347–361
Peterson PM, Romaschenko K, Johnson G (2010a) A classification of the Chloridoideae (Poaceae) based on multi-gene phylogenetic trees. Mol Phylogenet Evol 55:580–598
Qu L, Hancock JF (2001) Detecting and mapping repulsion-phase linkage in polyploids with polysomic inheritance. Theor Appl Genet 103:136–143
Rai PK, Jaiswal D, Rai DK, Sharma B, Watal G (2010) Antioxidant potential of oral feeding of *Cynodon dactylon* extract on diabetes-induced oxidative stress. J Food Biochem 34:78
Razmjoo K, Adavi Z (2012) Assessment of bermudagrass cultivars for phytoremediation of petroleum contaminated soils. Int J Phytoremediation 14:14–23
Ripol MI, Churchill GA, Silva JAGd, Sorrells M (1999) Statistical aspects of genetic mapping in autopolyploids. Gene 235:31–41
Robinson BP, Latham JM (1956) Tifgreen-an improved turf Bermuda grass. US Golf Ass J 9:26–28
Rousseau-Gueutin M, Lerceteau-Köhler E, Barrot L, Sargent DJ, Monfort A, Simpson D, Arús P, Guérin G, Denoyes-Rothan B (2008) Comparative genetic mapping between octoploid and diploid *Fragaria* species reveals a high level of colinearity between their genomes and the essentially disomic behavior of the cultivated octoploid strawberry. Genetics 179:2045–2060
Scalfi M, Troggio M, Piovani P, Leonardi S, Magnaschi G, Vendramin GG, Menozzi P (2004) A RAPD, AFLP and SSR linkage map, and QTL analysis in European beech (*Fagus sylvatica* L.). Theor Appl Genet 108:433–441
Schie S, Chaudhary R, Debener T (2014) Analysis of a complex polyploid plant genome using molecular markers: strong evidence for segmental allooctoploidy in garden dahlias. Plant Genome 7(3) doi:10.3835/plantgenome2014.01.0002
Silva JAGd, Sorrells ME, Burnquist WL, Tanksley SD (1993) RFLP linkage map and genome analysis of *Saccharum spontaneum*. Genome 36:782–791
Soltis DE, Soltis PS (1999) Review: Polyploidy: recurrent formation and genome evolution. Trends Ecol Evol 14:348–352
Soltis PS, Liu XX, Marchant DB, Visger CJ, Soltis DE (2014) Polyploidy and novelty: Gottlieb's legacy. Philos Trans R Soc Lond Ser B Biol Sci 369:20130351–20130351
Soreng RJ, Peterson PM, Romaschenko K, Davidse G, Zuloaga FO, Judziewicz EJ, Filgueiras TS, Davis JI, Morrone O (2015) A worldwide phylogenetic classification of the Poaceae (Gramineae). J Syst Evol 53:117–137
Sorrells ME (1992) Development and application of RFLPs in polyploids. Crop Sci 32:1086–1091
Souza LM, Mantello CC, Suzuki F, Gazaffi R, Garcia D, Le Guen V, Garcia AAF, Souza AP (2011) Development of a genetic linkage map of rubber tree (*Hevea braziliensis*) based on microsatellite markers. BMC Proc 5:1–2
Srinivasachary, Dida M, Gale M, Devos K (2007) Comparative analyses reveal high levels of conserved colinearity between the finger millet and rice genomes. Theor Appl Genet 115:489–499
Stebbins GLJ (1947) Types of polyploids: their classification and significance. Adv Genet 1:403–429
Stift M, Berenos C, Kuperus P, van Tienderen PH (2008) Segregation models for disomic, tetrasomic and intermediate inheritance in tetraploids: a general procedure applied to Rorippa (yellow cress) microsatellite data. Genetics 179:2113–2123
Sybenga J (1994) Preferential pairing estimates from multivalent frequencies in tetraploids. Genome / National Research Council Canada = Génome / Conseil National De Recherches Canada 37:1045–1055
Sybenga J (1996) Chromosome pairing affinity and quadrivalent formation in polyploids: do segmental allopolyploids exist? Genome 39:1176–1184
Taliaferro CM, Hopkins AA, Henthorn JC, Murphy CD, Edwards RM (1997) Use of flow cytometry to estimate ploidy level in *Cynodon* species. Int Turfgrass Soc Res J 8:385–392
Tan C, Wu Y, Taliaferro CM, Bell GE, Martin DL, Smith MW, Moss JQ (2014) Selfing and outcrossing fertility in common bermudagrass under open-pollinating conditions examined by SSR markers. Crop Sci 54:1832–1837
Tanaka H, Hirakawa H, Kosugi S, Nakayama S, Ono A, Watanabe A, Hashiguchi M, Gondo T, Ishigaki G, Muguerza M, Shimizu K, Sawamura N, Inoue T, Shigeki Y, Ohno N, Tabata S, Akashi R, Sato S (2016) Sequencing and comparative analyses of the genomes of zoysiagrasses. DNA Res 1–10. doi:10.1093/dnares/dsw006
Voorrips RE (2002) MapChart: software for the graphical presentation of linkage maps and QTLs. J Hered 93:77–78
Wang FF, Singh R, Genovesi AD, Wai CM, Huang X, Chandra A, Yu QY (2015a) Sequence-tagged high-density genetic maps of *Zoysia japonica* provide insights into genome evolution in Chloridoideae. Plant J 82:744–757
Wang X, Jin D, Wang Z, Guo H, Zhang L, Wang L, Li J, Paterson AH (2015b) Telomere-centric genome repatterning determines recurring chromosome number reductions during the evolution of eukaryotes. New Phytol 205:378–389
Wu Y (2011) Cynodon. In: Kole C (ed) Wild Crop relatives: genomic and breeding resources. Springer, Berlin, pp 53–71
Wu KK, Burnquist W, Sorrells ME, Tew TL, Moore PH, Tanksley SD (1992) The detection and estimation of linkage in polyploids using single-dose restriction fragments. Theor Appl Genet 83:294–300

Wu RL, Han YF, Hu JJ, Fang JJ, Li L, Li ML, Zeng ZB (2000) An integrated genetic map of *Populus deltoides* based on amplified fragment length polymorphisms. Theor Appl Genet 100:1249–1256

Wu R, Ma CX, Painter I, Zeng ZB (2002) Simultaneous maximum likelihood estimation of linkage and linkage phases in outcrossing species. Theor Popul Biol 61:349–363

Wu J, Jenkins J, Zhu J, McCarty J, Watson C (2003) Monte Carlo simulations on marker grouping and ordering. Theor Appl Genet 107:568–573

Wu YQ, Taliaferro CM, Bai GH, Anderson MP (2004) AFLP analysis of *Cynodon dactylon* (L.) Pers. var. *dactylon* genetic variation. Genome 47:689–696

Wu YQ, Taliaferro CM, Bai GH, Martin DL, Anderson JA, Anderson MP, Edwards RM (2006) Genetic analyses of Chinese *Cynodon* accessions by flow cytometry and AFLP markers. Crop Sci 46:917–926

Wu Y, Close TJ, Lonardi S (2011) Accurate construction of consensus genetic maps via integer linear programming. IEEE/ACM Trans Comput Biol Bioinform IEEE ACM 8:381–394

Xu J, Wang Z, Cheng JJ (2011) Bermuda grass as feedstock for biofuel production: a review. Bioresour Technol 102:7613–7620

Yin T, Huang M, Wang M, Zhu L-H, Zeng Z-B, Wu R (2001) Preliminary interspecific genetic maps of the *Populus* genome constructed from RAPD markers. Genome 44:602–609

Zeid M, Belay G, Mulkey S, Poland J, Sorrells ME (2011) QTL mapping for yield and lodging resistance in an enhanced SSR-based map for tef. Theor Appl Genet 122(1):77–93

Zhiyong W, Li L, Xuejun Y, Hailin G, Aigui G, Jianxiu L (2013) Genetic diversity analysis of *Cynodon dactylon* (bermudagrass) accessions and cultivars from different countries based on ISSR and SSR markers. Biochem Syst Ecol 46:108–115